JOC Article

3,5,7,9-Substituted Hexaazaacridines: Toward Structures with Nearly Degenerate Singlet−Triplet Energy Separations

Peter Langer,*[,||,‡] Shadi Amiri,[§] Anja Bodtke,[¶] Nehad N. R. Saleh,[||] Klaus Weisz,[#] Helmar Görls,[⊥] and Peter R. Schreiner*[,§]

Institut für Chemie, Universität Rostock, Albert-Einstein-Str. 3a, D-18059 Rostock, Germany, Leibniz-Institut für Katalyse e. V. an der Universität Rostock, Albert-Einstein-Str. 29a, D-18059 Rostock, Germany, Institut für Organische Chemie, Justus-Liebig-Universität Giessen, Heinrich-Buff-Ring 58, D-35392 Giessen, Germany, Institut für Pharmazie, Universität Greifswald, Friedrich-Ludwig-Jahn-Str. 17, D-17487 Greifswald, Germany, Institut für Biochemie, Universität Greifswald, Felix-Hausdorff-Str. 18, D-17467 Greifswald, Germany, and Institut für Anorganische and Analytische Chemie, Universität Jena, August-Bebel-Str. 2, 07740 Jena, Germany

peter.langer@uni-rostock.de; prs@org.chemie.uni-giessen.de

Received March 24, 2008

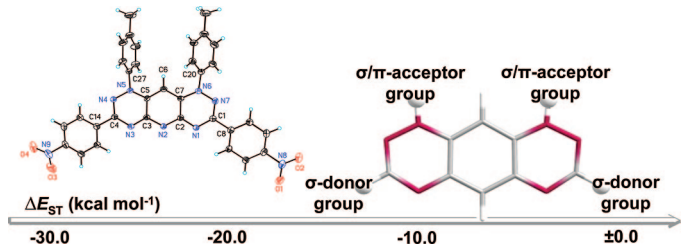

Toward the goal of preparing stable, neutral open-shell systems, we synthesized a novel series of *p*-phenyl-substituted 3,5,7,9-hexaazaacridine and 3,5,7,9-hexaazaanthracene derivatives. The effects of substitution on the molecular electronic properties were probed both experimentally and computationally [B3LYP/6-311G(d,p)//B3LYP/6-31G(d,p)]. While the experimentally prepared structures already have small (20−25 kcal/mol) singlet−triplet energy gaps, systems with even smaller (<9 kcal/mol) singlet−triplet energy separations can be realized through systematic variation of the substituent numbers, types, and patterns. Hexaazaanthracenes show generally smaller singlet−triplet energy gaps than hexaazaacridines. Nitrogen-bonded σ- and π-acceptor substituents that cause positive inductive and mesomeric effects as well as carbon-bonded σ-donor substituents make substituted hexaazaanthracenes promising candidates for purely organic high-spin systems.

Introduction

Paramagnetic single molecules represent attractive building blocks for the development of ferro- and ferrimagnetic materials.[1] The first purely organic ferromagnet was reported in 1991 by Kinoshita et al. who found that *p*-nitrophenyl nitronyl nitroxide radicals exhibit intermolecular ferromagnetic interactions in a β-phase crystal at 0.60 K.[2] This structure was modified by Pratt and Blundell et al. to increase the ferromagnetic coupling through the intermolecular SOMO interactions in the crystalline state.[3] Research on molecules with promising electronic structures for potential applications in organic magnetism as well as organic electronics includes open-shell ground state systems or materials with small singlet−triplet energy separations (ΔE_{ST}), as these may be valuable magnetic materials in their ground or optically excited states.

In recent years, particular attention has been paid to tetrathiafulvalenes (TTFs),[4] carbenes,[5] fullerenes,[6] oligoacenes,[7] and related species. The synthetic availability of compounds with

[||] Universität Rostock.
[‡] Leibniz-Institut für Katalyse e. V. an der Universität Rostock.
[§] Justus-Liebig-Universität Giessen.
[¶] Institut für Pharmazie, Universität Greifswald.
[#] Institut für Biochemie, Universität Greifswald.
[⊥] Universität Jena.

(1) Aubin, S. M. J.; Wemple, M. W.; Adams, D. M.; Tsai, H.-L.; Christou, G.; Hendrickson, D. N. *J. Am. Chem. Soc.* **1996**, *118*, 7746.

(2) Tamura, M.; Nakazawa, Y.; Shiomi, D.; Nozawa, K.; Hosokoshi, Y.; Ishikawa, M.; Takahashi, M.; Kinoshita, M. *Chem. Phys. Lett.* **1991**, *186*, 401.

(3) (a) Pratt, F. L.; Valladares, R.; Caulfield, J.; Deckers, I.; Singleton, J.; Fisher, A. J.; Hayes, W.; Kurmoo, M.; Day, P.; Sugano, T. *Synth. Met.* **1993**, *61*, 171. (b) Blundell, S. J.; Marshall, I. M.; Lovett, B. W.; Pratt, F. L.; Hayes, W.; Kurmoo, M.; Takagi, S.; Sugano, S. *Hyperfine Interact.* **2001**, *133*, 169.

10.1021/jo8005123 CCC: $40.75 © 2008 American Chemical Society
Published on Web 05/22/2008

such unusual magnetic and/or electronic properties is crucial for their further development. Triplet carbenes have been considered as candidates for organic magnetic materials,[8] but their typically high reactivities make them difficult to handle and to isolate. A recent theoretical study by Woodcock et al. including an empirical correction showed that the big aryl substituents such as 1-naphthyl[9] and 9-anthryl groups[10] reduce ΔE_{ST} of carbenes effectively due to increased resonance stabilization, and this reduction is more pronounced for the 9-anthryl group due to its exceptional ability to resonance stabilize the triplet state than singlet state.[11]

Heterocyclic thiazyl radicals with an unpaired electron belong to a family of molecules with the potential for application as organic ferromagnets.[12,13] The most pursued candidates contain five-membered rings, as shown in Scheme 1. The band gaps of these molecules are very sensitive to their substitution pattern.[14] The electronic and magnetic properties of the analogous six-membered ring systems (Scheme 1) are less well-characterized because of their tendency to dimerize (formation of S−S bonds).[15] Recently, Leitch et al.[16] introduced the first examples of π-stacked bisthiadiazinyl radicals (**1**) as a new class of neutral heterocyclic π-radicals that are monomeric in the solid state; these radicals derive their stabilization from resonance effects.[17] Replacing sulfur with selenium in these species increases intermolecular interactions and hence causes a marked increase in conductivity.[18] Another remarkable example is the bulk ferromagnetism of bisthiaselenazolyl **1c** with an ordering temperature (T_c) of 12.3 K.[12a]

SCHEME 1. Thiazyl Radicals

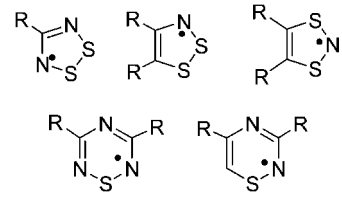

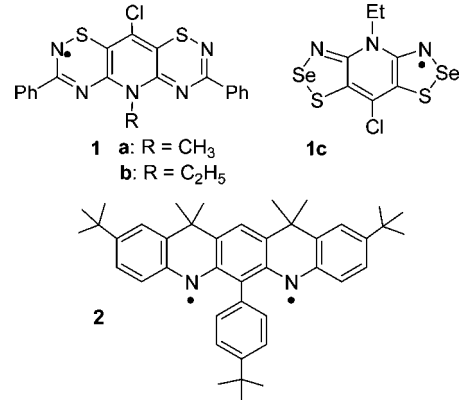

To date, only a small number of isolated stable neutral single organic molecules with at least a triplet ground state ($S \geq 1$) as high-spin organics have been reported. Recently, the first established triplet ground state aminyl diradical (**2**) with strong ferromagnetic coupling was presented by Rajca et al.[19]

Linear polycyclic aromatic hydrocarbons (PAHs) composed of fused benzene rings (oligoacenes) display small ΔE_{ST} values. The higher members of the oligoacenes were predicted to have rather small ΔE_{ST} values and potentially open-shell singlet character.[7d,20] These systems are computationally difficult because the wave functions of oligoacenes larger than hexacene are not stable.[7g,h] Likewise, the preparation of oligoacenes larger

(4) (a) Clemente-Leon, M.; Coronado, E.; Galan-Mascaros, J. R.; Gomez-Garcia, C. J.; Rovira, C.; Lauhkin, V. N. *Synth. Met.* **1999**, *103*, 2339. (b) Perepichka, D. F.; Bryce, M. R.; Pearson, C.; Petty, M. C.; McInnes, E. J. L.; Zhao, J. P. *Angew. Chem., Int. Ed.* **2003**, *42*, 4636. (c) Ribas, X.; Mas-Torrent, M.; Perez-Benitez, A.; Dias, J. C.; Alves, H.; Lopes, E. B.; Henriques, R. T.; Molins, E.; Santos, I. C.; Wurst, K.; Foury-Leylekian, P.; Almeida, M.; Veciana, J.; Rovira, C. *Adv. Funct. Mater.* **2005**, *15*, 1023. (d) Nielson, M. B.; Lomholt, C.; Becher, J. *Chem. Soc. Rev.* **2000**, *29*, 153. (e) Bryce, M. R. *Adv. Mater.* **1999**, *11*, 11.

(5) (a) Schreiner, P. R.; Reisenauer, H. P. *ChemPhysChem* **2006**, *7*, 880. (b) Nemirowski, A.; Reisenauer, H. P.; Schreiner, P. R. *Chem.—Eur. J.* **2006**, *12*, 7411. (c) Schreiner, P. R. *J. Am. Chem. Soc.* **1998**, *120*, 4184. (d) Hirai, K.; Tomioka, H. *J. Am. Chem. Soc.* **1999**, *121*, 10213. (e) Itoh, T.; Jinbo, Y.; Hirai, K.; Tomioka, H. *J. Am. Chem. Soc.* **2005**, *127*, 1650.

(6) (a) Narymbetov, B.; Omerzu, A.; Kabanov, V. V.; Tokumoto, M.; Kobayashi, H.; Mihailovic, D. *Nature* **2000**, *407*, 883. (b) Blinc, R.; Jeglic, P.; Apih, T.; Seliger, J.; Arcon, D.; Omerzu, A. *Phys. Rev. Lett.* **2002**, *88*, 86402/1. (c) Gotschy, B. *Phys. Rev. B* **1995**, *52*, 7378.

(7) (a) Langer, P.; Bodtke, A.; Saleh, N. N. R.; Görls, H.; Schreiner, P. R. *Angew. Chem., Int. Ed.* **2005**, *44*, 5255. (b) Anthony, J. E. *Chem. Rev.* **2006**, *106*, 5028. (c) Nunzi, F.; Ruiz, E.; Cano, J.; Alvarez, S. *J. Phys. Chem. C* **2007**, *111*, 618. (d) Sanchez-Carrera, R. S.; Coropceanu, V.; da Silva Filho, D. A.; Friedlein, R.; Osikowicz, W.; Murdey, R.; Suess, C.; Salaneck, W. R.; Bredas, J.-L. *J. Phys. Chem. B* **2006**, *110*, 18904. (e) Dos Santos, M. C *Phys. Rev. B* **2006**, *74*, 45426/1. (f) Hummer, K; Ambrosch-Draxl, C. *Phys. Rev. B* **2005**, *72*, 205205/1. (g) Bendikov, M.; Wudl, F.; Perepichka, D. F. *Chem. Rev.* **2004**, *104*, 4891. (h) Schleyer, P. v. R.; Manoharan, M.; Jiao, H.; Stahl, F. *Org. Lett.* **2001**, *3*, 3643.

(8) (a) Itoh, T.; Takada, A.; Hirai, K.; Tomioka, H. *Org. Lett.* **2005**, *7*, 811. (b) Nicolaides, A.; Enyo, T.; Miura, D.; Tomioka, H. *J. Am. Chem. Soc.* **2001**, *123*, 2628. (c) Despagnet-Ayoub, E.; Sole, S.; Gornitzka, H.; Rozhenko, A. B.; Schoeller, W. W.; Bourissou, D.; Bertrand, G. *J. Am. Chem. Soc.* **2003**, *125*, 124. (d) Woodcock, H. L.; Moran, D.; Schleyer, P. v. R.; Schaefer, H. F. *J. Am. Chem. Soc.* **2001**, *123*, 4331.

(9) (a) Trindle, C. *J. Org. Chem.* **2003**, *68*, 9669. (b) Tomioka, H.; Iwamoto, E.; Itakura, H.; Hirai, K. *Nature* **2001**, *412*, 626.

(10) (a) Yoshida, K.-I.; Iiba, E.; Nozaki, Y.; Hirai, K.; Takahashi, Y.; Tomioka, H.; Lin, C.-T.; Gaspar, P. P. *Bull. Chem. Soc. Jpn.* **2004**, *77*, 1509. (b) Trindle, C. *J. Org. Chem.* **2003**, *68*, 9669. (c) Tsuchiya, Y.; Matsuno, M.; Itoh, T.; Hirai, K.; Tomioka, H. *Bull. Chem. Soc. Jpn.* **2005**, *78*, 2037. (d) Yoshida, K.-I.; Iiba, E.; Nozaki, Y.; Hirai, K.; Takahashi, Y.; Tomioka, H.; Lin, C.-T; Gaspar, P. P. *Bull. Chem. Soc. Jpn.* **2004**, *77*, 1509. (e) Takahashi, Y.; Tomura, M.; Yoshida, K.-I.; Murata, S.; Tomioka, H. *Angew. Chem., Int. Ed.* **2000**, *39*, 3478.

(11) Woodcock, H. L.; Moran, D.; Brooks, B. R.; Schleyer, P. v. R.; Schaefer, H. F. *J. Am. Chem. Soc.* **2007**, *129*, 3763.

(12) (a) Robertson, C. M.; Myles, D. J. T.; Leitch, A. A.; Reed, R. W.; Dooley, B. M.; Frank, N. L.; Dube, P. A.; Thompson, L. K.; Oakley, R. T. *J. Am. Chem. Soc.* **2007**, *129*, 12688. (b) Alberola, A.; Less, R. J.; Pask, C. M.; Rawson, J. M.; Palacio, F.; Oliete, P.; Paulsen, C.; Yamaguchi, A.; Farley, R. D.; Murphy, D. M. *Angew. Chem., Int. Ed.* **2003**, *42*, 4782.

(13) (a) Awaga, K.; Tanaka, T.; Shirai, T.; Fujimori, M.; Suzuki, Y.; Yoshikawa, H.; Fujita, W. *Bull. Chem. Soc. Jpn.* **2006**, *79*, 25. (b) Mito, M.; Fujino, M.; Deguchi, H.; Takagi, S.; Fujita, W.; Awaga, K. *Polyhedron* **2005**, *24*, 2501.

(14) (a) Barclay, T. M.; Cordes, A. W.; George, N. A.; Haddon, R. C.; Itkis, M. E.; Mashuta, M. S.; Oakley, R. T.; Patenaude, G. W.; Reed, R. W.; Richardson, J. F.; Zhang, H. *J. Am. Chem. Soc.* **1998**, *120*, 352. (b) Cordes, A. W.; Minge, J. R.; Oakley, R. T.; Reed, R. W.; Zhang, H. *Can. J. Chem.* **2001**, *79*, 1352. (c) Brusso, J. L.; Clements, O. P.; Haddon, R. C.; Itkis, M. E.; Leitch, A. A.; Oakley, R. T.; Reed, R. W.; Richardson, J. F. *J. Am. Chem. Soc.* **2004**, *126*, 8256.

(15) (a) Hayes, P. J.; Oakley, R. T.; Cordes, A. W.; Pennington, W. T. *J. Am. Chem. Soc.* **1985**, *107*, 1346. (b) Zienkiewicz, J.; Kaszynski, P.; Young, V. G., Jr *J. Org. Chem.* **2004**, *69*, 7525.

(16) Leitch, A. A.; Oakley, R. T.; Reed, R. W.; Thompson, L. K. *Inorg. Chem.* **2007**, *46*, 6261.

(17) (a) Beer, L.; Brusso, J. L.; Cordes, A. W.; Haddon, R. C.; Itkis, M. E.; Kirschbaum, K.; MacGregor, D. S.; Oakley, R. T.; Pinkerton, A. A.; Reed, R. W. *J. Am. Chem. Soc.* **2002**, *124*, 9498. (b) Beer, L.; Brusso, J. L.; Haddon, R. C.; Itkis, M. E.; Oakley, R. T.; Reed, R. W.; Richardson, J. F.; Secco, R. A.; Yu, X. *Chem. Commun.* **2005**, *46*, 5745. (c) Brusso, J. L.; Derakhshan, S.; Itkis, M. E.; Kleinke, H.; Haddon, R. C.; Oakley, R. T; Reed, R. W.; Richardson, J. F.; Robertson, C. M.; Thompson, L. K. *Inorg. Chem.* **2006**, *45*, 10958.

(18) Beer, L.; Brusso, J. L.; Haddon, R. C.; Itkis, M. E.; Kleinke, H.; Leitch, A. A.; Oakley, R. T.; Reed, R. W.; Richardson, J. F.; Secco, R. A.; Yu, X. *J. Am. Chem. Soc.* **2005**, *127*, 18159.

(19) Rajca, A.; Shiraishi, K.; Pink, M.; Rajca, S. *J. Am. Chem. Soc.* **2007**, *129*, 7232.

than hexacene has not yet been accomplished, due to their unstable nature (facile oxidation and dimerization).[20,21]

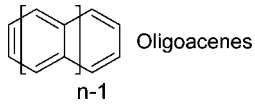

Oligoazaacenes represent analogues of oligoacenes in which some sp^2 carbon moieties (CH) are substituted with nitrogen atoms. Recently, Winkler and Houk investigated this class of compounds computationally and found that oligoazaacenes generally have ΔE_{ST} values smaller than those of their all-carbon analogues.[22] Recent progress in the chemistry of polyazaacenes includes new strategies for their preparation.[23]

3,5,7,9-Tetraphenylhexaazaanthracene (TPH-anthracene, **4a**) was found to have a singlet ground state resulting in a zwitterionic structure with a ΔE_{ST} of about 19 kcal mol^{-1};[24] **4a** undergoes photoinduced intramolecular electron transfer to give a radical pair.[25] The electronically related azaacene 5,7-diphenyl-5*H*,12*H*-quinoxalino[2,3-*b*]phenazine (**5a**) also possesses a singlet ground state with a pronounced zwitterionic structure.[26] Tetraazapentacenes with long-chain alkyl substituents (**5b** and **5c**) have molecular structures that promote a range of possible packing configurations because of their zwitterionic character.[27]

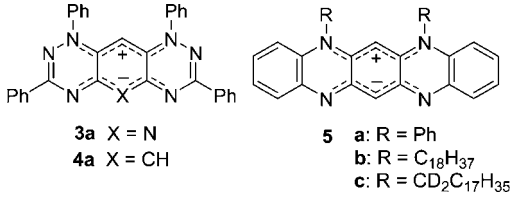

We reported recently the synthesis and characterization of 3,5,7,9-tetraphenylhexaazaacridine (TPH-acridine, **3a**), which again exists as a zwitterion rather than as a diradical (Scheme 2).[7a] In agreement with the experimental findings, density functional theory (DFT) computations characterize both **3a** and **4a** as highly zwitterionic structures with very low-lying triplet states. These structures can be considered as rare cases of stable 16 π-electrons, weakly antiaromatic entities. The present paper focuses on the synthesis and properties of substituted hexaazaacridines and hexaazaanthracenes. These molecules combine an unusual stability with low-lying electronic triplet states.

We systematically explore substituent effects on the way to the development of molecules with small ΔE_{ST} values or even a triplet ground state. The ultimate goal would be the identification of stable open-shell structures that may be candidates for magnetic materials. Of course, we currently cannot predict the ability of these structures with respect to the coupling of their individual spins as this is a macroscopic property. In the following, we present a combined experimental and computational study on the preparation and characterization of novel TPH-acridines and TPH-anthracenes. Systematic computations on the substituent effects help explain the electronic properties of the prepared compounds and are used to predict ways to minimize the ΔE_{ST} values.

SCHEME 2. TPH-Acridine in Zwitterionic Ground and Photoexcited Triplet States

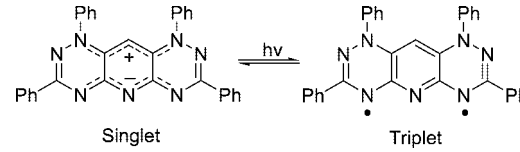

Results and Discussion

A. Synthesis. The synthesis of 3,5,7,9-tetraphenylhexaazaacridines **3a**−**i** was not straightforward, and the protocol of all steps had to be thoroughly optimized for each individual derivative (Scheme 3 and Table 1). The reaction of 2,6-diaminopyridine with aromatic acid chlorides afforded the bis(amides) **6a**−**f** which were transformed into the bis(imidoyl) dichlorides **7a**−**f**. The condensation of phenyl- and tolylhydrazine with **7a**−**f** gave the amidrazones **8a**−**i**, which were transformed into the 3,5,7,9-tetraphenylhexaazaacridines **3a**−**i** by oxidative cyclization (DBU, air, MeOH, or EtOH).

The (optimized) yields of acridines **3a**−**i** are based on the corresponding bis(amides) **6a**−**f** and are in the range of 6−27%; the best yields were obtained for acridines **3d**, **3h**, and **3i**. During the optimization, the high purity of **7a**−**f**, the reaction time of the final cyclization step, and the workup and purification for

SCHEME 3. Synthesis of 3,5,7,9-Tetraphenylhexaazaacridines 3a−i[a]

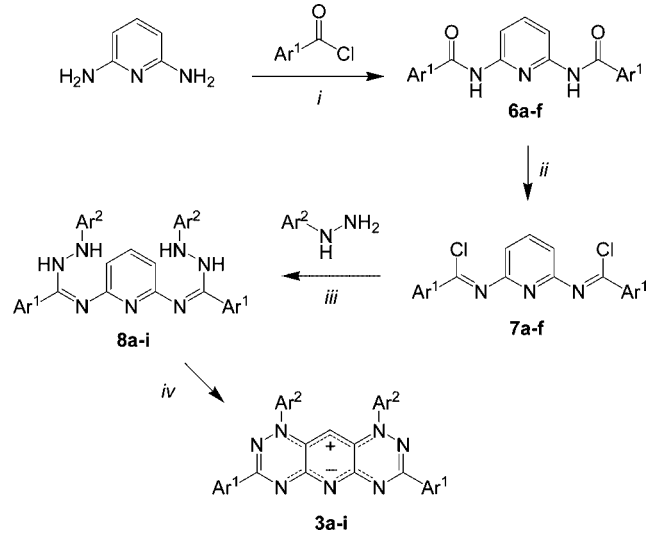

[a] Conditions: (*i*) Ar^1COCl (2 equiv), NEt_3 (2 equiv), CH_2Cl_2, 14 h, 0−20 °C; (*ii*) PCl_5 (2.9 equiv.), toluene, 1.5 h, 20 °C, then 2 h, 110 °C, 88%; (*iii*) Ar^2NHNH_2 (2.7 equiv), *n*-hexane, 14 h, 0−20 °C (in some cases, NEt_3 was added, see Supporting Information); (*iv*) air, DBU (2.8 equiv), MeOH (for **3h,i**: EtOH), 4−14 h, 20 °C.

(20) (a) Anthony, J. E. *Angew. Chem., Int. Ed.* **2007**, *46*, 2. (b) Lowe, J. P.; Kafafi, S. A.; LaFemina, J. P. *J. Phys. Chem.* **1986**, *90*, 6602. (c) Kivelson, S.; Chapman, O. L. *Phys. Rev. B* **1983**, *28*, 7236. (d) Houk, N. K.; Lee, P. S.; Nendel, M. *J. Org. Chem.* **2001**, *66*, 5517. (e) Kao, J.; Lilly, A. C., Jr. *J. Am. Chem. Soc.* **1987**, *109*, 4149. (f) Ali, Md. E.; Datta, S. N. *J. Phys. Chem. A* **2006**, *110*, 13232.

(21) Payne, M. M.; Parkin, S. R.; Anthony, J. E. *J. Am. Chem. Soc.* **2005**, *127*, 8028.

(22) Winkler, M.; Houk, K. N. *J. Am. Chem. Soc.* **2007**, *129*, 1805.

(23) Stöckner, F; Beckert, R.; Gleich, D.; Birckner, E; Günther, W; Görls, H.; Vaughan, G *Eur. J. Org. Chem.* **2007**, 1237.

(24) Hutchison, K.; Srdanov, G.; Hicks, R.; Yu, H.; Wudl, F.; Strassner, T.; Nendel, M.; Houk, K. N. *J. Am. Chem. Soc.* **1998**, *120*, 2989.

(25) (a) Hutchison, K. A.; Hasharoni, K.; Wudl, F.; Berg, A.; Shuali, Z.; Levanon, H. *J. Am. Chem. Soc.* **1998**, *120*, 6362. (b) Braunstein, P.; Siri, O.; Taquet, J.-p.; Rohmer, M.-M.; Benard, M.; Welter, R. *J. Am. Chem. Soc.* **2003**, *125*, 12246.

(26) Wudl, F.; Koutentis, P. A.; Weitz, A.; Ma, B.; Strassner, T.; Houk, K. N.; Khan, S. I. *Pure Appl. Chem.* **1999**, *71*, 295.

(27) Choi, H.; Yang, X.; Mitchell, G. W.; Collier, C. P.; Wudl, F.; Heath, J. R. *J. Phys. Chem. B* **2002**, *106*, 1833.

TABLE 1. Yields and Selected NMR Data of Acridines 3a−i

6	3	Ar^1	Ar^2	% 6[a]	% 3[b]	^{1}H NMR[d]
a	**a**	Ph	Ph	48	23[b], 30[c]	5.75
a	**b**	Ph	*p*-MeC_6H_4	48	14	5.85
b	**c**	*p*-MeC_6H_4	Ph	62	6	5.88
c	**d**	*p*-ClC_6H_4	Ph	54	23	5.68
c	**e**	*p*-ClC_6H_4	*p*-MeC_6H_4	54	11	5.73
d	**f**	*p*-$NO_2C_6H_4$	Ph	62	14	5.63
d	**g**	*p*-$NO_2C_6H_4$	*p*-MeC_6H_4	62	11	5.69
e	**h**	naphth-2-yl	Ph	70	21	5.54
f	**i**	pyrid-4-yl	Ph	49	27	5.68

[a] Yields of isolated products. [b] Yields based on **6**. [c] Yield based on **8a**. [d] Central acridine proton or carbon (TFA-d_1).

each individual acridine derivative (see Supporting Information) proved to be important parameters. In addition, it also proved to be very important to use the bis(imidoyl) dichlorides **7** and bis(amidrazones) **8** immediately after their preparation. Imidoyl chlorides **7** were not recrystallized but were carefully dried. Bis(amidrazones) **8** could not be dried completely because they tend to decompose upon drying and standing. The amounts of the reagents for the cyclization step were calculated based on a theoretical 100% yield of amidrazones **8**. With regard to our previous synthesis of **3a**,[7a] we were able to optimize the yield of the cyclization reaction from 10 to 30% and the overall yield (based on bis(amide) **6a**) from 8 to 23%.

For reasons of comparison, the novel zwitterionic TPH-anthracene **4b** (10% yield) was prepared from 1,3-diaminobenzene following the procedure as given for the synthesis of acridines **3a-i**. Anthracene **4b** represents the carba-analogue of acridine derivative **3c**. Anthracene **4a** (the analogue of **3a**) was prepared following the procedure reported by Wudl and co-workers. In contrast to these authors, we have been able to isolate pure **4a**, despite much synthetic efforts, in only 7% yield.

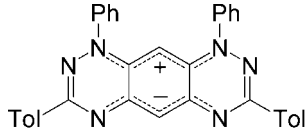

4b Tol = *p*-MeC_6H_4

B. Absorption and Fluorescence. Acridines **3a−i** are red to deep red solids, atmosphere as well as thermally stable, and poorly soluble in DMF, CH_2Cl_2, acetonitrile, and toluene. Acridine **3a** is also poorly soluble in concentrated nitric acid (red solution), phosphoric acid (blue-purple solution), perchloric acid (green solution), and acetic acid (orange solution). In contrast, **3a** is reasonably soluble in TFA (deep purple solution), which can be explained by the formation of cation **3aH**$^+$. An X-ray crystal structure analysis of **3aH**$^+$ revealed that the protonation occurred at the central nitrogen atom and that the cation resides in the form of resonance structure **A** (Scheme 4).[7a]

Excellent solubility and a strong bathochromic effect is observed in concentrated sulfuric acid (λ_{max} = 662 nm, deep green solution). The bathochromism can be explained by complete protonation of the acridine, formation of aggregates (vide infra), and the influence of the counterion. A solvatochromic effect, depending on the polarity of the solvent,[28] is observed for all acridines **3a−i** and for anthracene **4b** (Table 2 and Figure 1). The solvatochromism of anthracene **4b** is more pronounced than that for acridine **3c** (which bears the same substituents). The absorptions of anthracene **4b** show a significant bathochromic shift compared to those of acridines **3a−i**. The influence of the substituents on the absorptions of acridines **3a−i** is relatively small. In DMF, a bathochromic shift is observed for acceptor-substituted acridines, whereas the absorptions of **3a−c** are in the range of λ_{max} = 547−548 nm, the absorptions of nitro derivatives **3f** and **3g** are λ_{max} = 587 and 589 nm, respectively (which is, in fact, close to the absorption of anthracene **4b**). A similar trend is observed for CH_2Cl_2, acetonitrile, and toluene but not for sulfuric, phosphoric, and acetic acid. Actually, in sulfuric acid, a hypsochromic effect is observed for **3f** and **3g** relative to **3a−c**. The orange colored DMF solution of acridine **3a** (λ_{max} = 547 nm) is highly fluorescent at $F\lambda_{max}$ = 585 nm. A shift of the fluorescence to higher wavelengths is observed for nitro-substituted acridines **3f** and **3g** ($F\lambda_{max}$ = 610 and 600 nm, respectively) and for anthracene **4b** ($F\lambda_{max}$ = 615 nm).

SCHEME 4. Resonance Structures of Protonated TPH-Acridines (3a−i)H$^+$

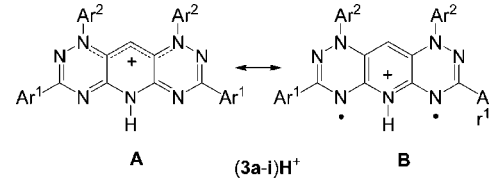

Figures 2 and 3 show the UV−vis absorption curves of acridines **3a** and **3d−i** and of anthracene **4b** in DMF and concentrated sulfuric acid, respectively. As discussed above, a bathochromic effect is observed for DMF solutions of **3f** and **4b** (Figure 2). Besides this effect, the UV−vis absorption curves are quite similar. The situation is different for solutions in concentrated sulfuric acid (Figure 3). Besides the bathochromic effect observed for **4b**, pyridine-substituted acridine **3i** displays a significant hypsochromic shift. This might be explained by competing protonation of the pyridine rather than the acridine nitrogen atoms.

Successive dilution of a solution of **3a** in concentrated sulfuric acid with water results in a change of color from deep green over blue and purple to pink and orange; this process is reversible (Figure 4 and Table 3). In fact, the addition of concd H_2SO_4 to a mixture of H_2SO_4/water = 1.5/2.55 resulted in a blue to green color. A similar solvatochromism was observed by dilution of a solution of **3a** in concentrated sulfuric acid with acetone (see Supporting Information). However, the solutions tend to be unstable at 20 °C.

Concentration-dependent UV−vis spectra of **3a** in CH_2Cl_2 did not show shifts of the maximum absorptions, and the Lambert−Beer law is valid for the 292 and 546 nm peaks within 4% error (Figure 5). Hence, there is no indication for the formation of aggregates. Cyclic voltammetry (CV) measurements were performed for **3a** in DMF containing Bu_4NClO_4 as supporting electrolyte; however, because of the low solubility, no peak current could be observed for this substrate.

C. Computational Analysis. To elucidate and understand the electronic structures of the prepared molecules in detail, we report in the following a systematic computational study on a large number of substituted hexaazaacridines and hexaazaanthracene analogues.

(28) Reichardt, C. *Solvents and Solvent Effects in Organic Chemistry*, 3rd ed.; Wiley-VCH: Weinheim, Germany, 2002.

TABLE 2. Solvatochromism (λ_{max} in nm) and Fluorescence of Acridines 3a−i

solvent	polarity[28]	3a	3b	3c	3d	3e	3f	3g	3h	3i	4b
H_2SO_4		662	*a*	685	667	681	631	649	663	558	719
H_3PO_4		540	*a*	654	*a*	537	538	537	*a*	529	655
HCO_2H	0.728	*a*	*a*	542	*a*	*a*	*a*	*a*	*a*	*a*	585
HOAc	0.648	535	538	542	538	539	534	536	546	521	568
MeCN	0.460	*a*	544	542	*a*	546	*a*	584	*a*	556	587
DMF	0.404	547	548	548	552	553	587	589	557	562	593
CH_2Cl_2	0.309	*a*	544	547	*a*	551	*a*	582	*a*	559	591
toluene	0.099	*a*	535	553	*a*	556	*a*	583	*a*	564	599
fluorescence		580	585	585	579	583	610	600	*a*	583	615
λ_{em} (λ_{ex}) DMF		(295)	(295)	(295)	(304)	(555)	(558)	(565)		(564)	(590)

[a] Not determined due to low solubility.

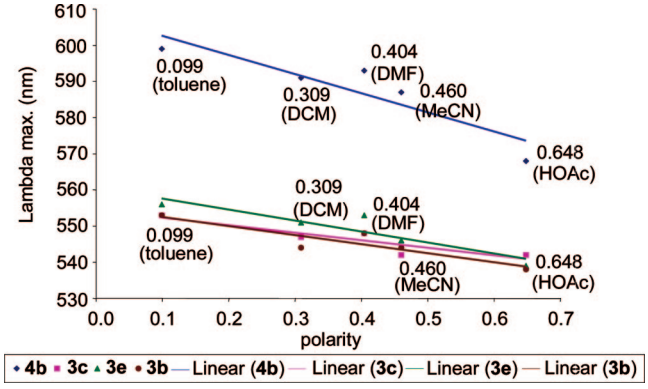

FIGURE 1. Absorption (λ_{max}) of acridines **3b**, **3c**, and **3e** and of anthracene **4b** in solvents with different polarities.

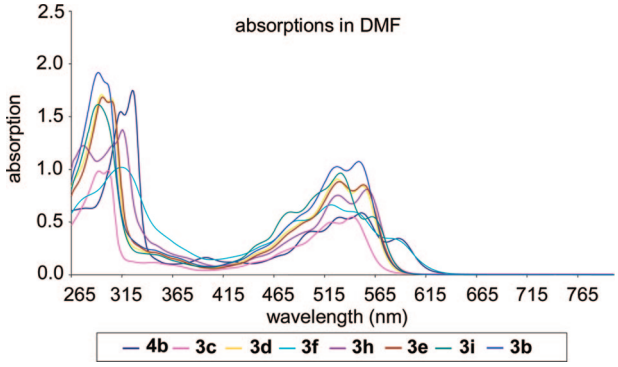

FIGURE 2. Absorptions of acridines **3b**−**f**, **3h**, and **3i** and of anthracene **4b** in DMF.

1. Computational Methods. Density functional theory (DFT) using Becke's three-parameter hybrid functional[29] (U)B3LYP with a 6-31G(d,p) basis set was employed to optimize all geometries and energies of singlet (spin-restricted wave functions) and triplet ground states (spin-unrestricted wave functions). Although open-shell singlet species are potentially also low-lying states,[30] we have shown recently that DFT methods are incapable of placing the energy of such states correctly, as exemplified with carbenes.[31] Therefore, we refrain from such computations; the singlet states would also be magnetically

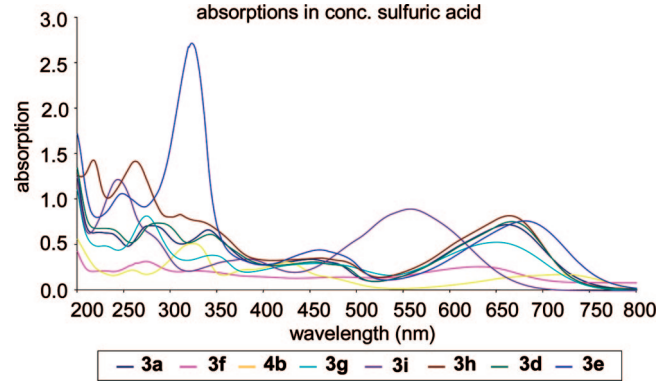

FIGURE 3. Absorptions of acridines **3a** and **3d**−**i** and of anthracene **4b** in concentrated sulfuric acid.

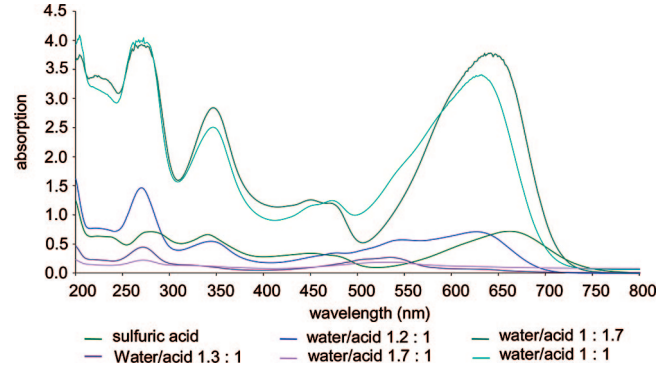

FIGURE 4. Solvatochromic effect of the dilution of a solution of **3a** in concentrated sulfuric acid (the colors of the curves represent the colors of the solutions).

TABLE 3. Solvatochromism of 3a in Concentrated H_2SO_4 /Water

H_2O/H_2SO_4	λ_{max} (nm)	color
0.0/1.0	662	deep green
1.0./1.7	641	green-blue
1.0/1.0	632	blue-green
1.2/1.0	626	blue
1.3/1.0	618	purple
1.7/1.0	534	pink

(29) (a) Becke, A. D. *J. Chem. Phys.* **1993**, *98*, 5648. (b) Becke, A. D. *Phys. Rev. A* **1988**, *38*, 3098.

(30) (a) Constantinides, C. P.; ; Koutentis, P. A.; ; Schatz, J. *J. Am. Chem. Soc.* **2004**, *126*, 16232. (b) Bendikov, M.; ; Duong, H. M.; ; Starkey, K.; ; Houk, K. N.; ; Carter, E. A.; ; Wudl, F. *J. Am. Chem. Soc.* **2004**, *126*, 7416. (c) Poater, J.; ; Bofill, J. M.; ; Alemany, P.; ; Sola, M. *J. Phys. Chem. A.* **2005**, *109*, 10629. (d) Chen, Z.; ; Jiang, D.; ; Lu, X.; ; Bettinger, H. F.; ; Dai, S.; ; Schleyer, P. v. R.; ; Houk, K. N. *Org. Lett.* **2007**, *9*, 5449. Note that it is rather unlikely that B3LYP/6-31G(d) gives a correct description of the open-shell singlet state. Figure 1 in this paper emphasizes this because the depicted energies are expected to decrease with *n*.

(31) Schreiner, P. R.; Reisenauer, H. P.; Allen, W. D.; Sattelmeyer, K. W. *Org. Lett.* **2004**, *6*, 1163.

(32) (a) Reddy, A. R.; Fridman-Marueli, G.; Bendikov, M. *J. Org. Chem.* **2007**, *72*, 51. (b) Reimers, J. R.; Hall, L. E.; Crossley, M. J.; Hush, N. S. *J. Phys. Chem. A* **1999**, *103*, 4385. (c) Poater, J.; Bofill, J. M.; Alemany, P.; Sola, M. *J. Phys. Chem. A* **2005**, *109*, 10629. (d) Portella, G.; Poater, J.; Bofill, J. M.; Alemany, P.; Sola, M. *J. Org. Chem.* **2005**, *70*, 2509.

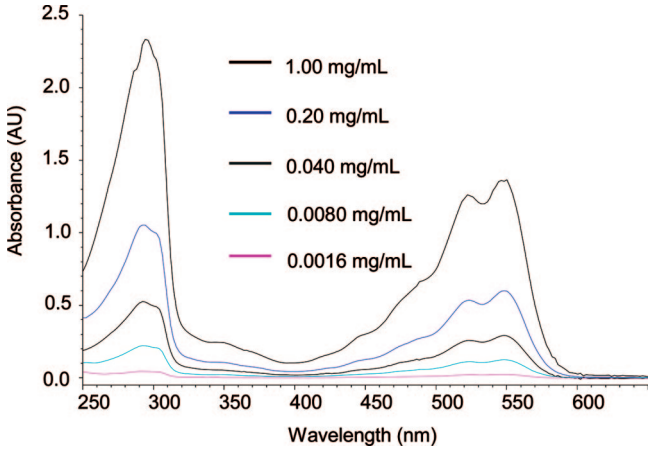

FIGURE 5. The concentration-dependent UV−vis spectra of **3a**.

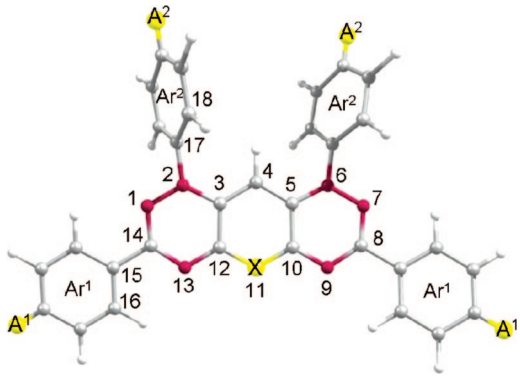

FIGURE 6. Generic structure of *para*-substituted TPH-anthracenes (X =CH) and TPH-acridines (X = N).

inactive. Previous results show that closed-shell singlet and triplet computations at this level of theory agree well with experiment for acenes[32] and azaacenes;[24,25,33] a generic structure is depicted in Figure 6. The computed vibrational frequencies show that all stationary points are minima, and zero-point vibrational energies (ZPVEs) are evaluated (no imaginary frequencies); the B3LYP/6-31G(d,p) wave functions of the parent systems **3a** and **4a** (both C_2 symmetric) are stable. The $<S^2>$ values of all singlet states were 0.00 and about 2.0 for the triplets.

Atomic charges were estimated at the same level of theory by using natural bond orbital analysis method (NBO 3.1). DFT was also utilized for NMR and nucleus-independent chemical shielding (NICS) computations with GIAO[34]-B3LYP/6-311G-(d,p) on the optimized geometries. NICS(0) and NICS(1) were determined as the negative value of the absolute isotropic magnetic shielding[35] with the SCGT[36]-DFT method (SCGT-B3LYP/6-311G(d,p)) by locating a ghost atom at the ring centers and at 1 Å above the plane of each ring. UV−vis spectra were evaluated with time-dependent DFT (TD-B3LYP/6-311G(d,p)). All computations employed the Gaussian03 program suite.[37]

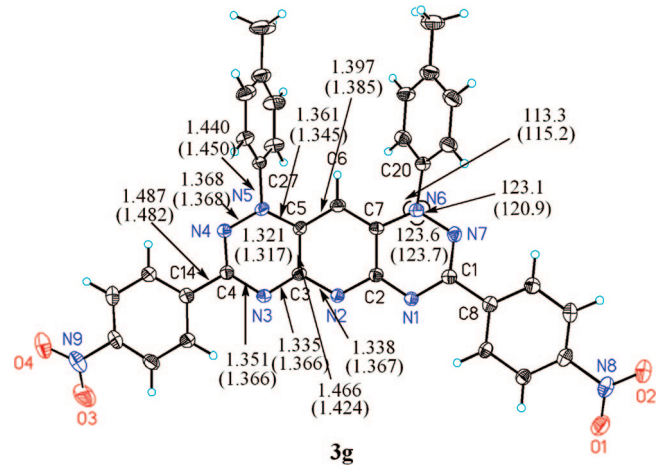

FIGURE 7. ORTEP drawing of **3g** with atom numbering. Comparison of experimental selected bond lengths (Å) and angles (°) (in parentheses) with averaged computational values [B3LYP/6-31G(d,p)].

2. Structure and Energies. The structural parameters computed for the minimum conformer of **3g** compare well with the X-ray crystal structure analyses (Figure 7). A high maximum peak and a low minimum hole in the difference were observed (0.792 and −0.696). These values are normal and correspond to less than one electron. The crystals were extremely thin and of low quality, resulting in a substandard data set; however, the structure is sufficient to show connectivity and geometry despite the high final *R* value. Although the effects of Peierls distortions for oligoacenes[20a,38] were indicated by Houk et al. and for polyacetylenes as well as cyanodienes[39] by Kato et al., the C−C bond lengths in the fused moieties show no Peierls distortion in the molecules under consideration here, and this emphasizes the notion of two delocalized nonalternating ribbons joined by two longer C−C bonds (∼1.42 Å, Figure 7). Also, the C^4−N^4 and C^1−N^7 bond lengths in the terminal rings (Figure 7) are short about the localized CN double bond and the π-density cannot be delocalized into the outer rings.

Natural charge analyses confirm that TPH-acridine and TPH-anthracene derivatives possess zwitterionic structures with negative partial charges in the bottom ribbon and partial positive charges in the top ribbon in their ground states (with an orientation as depicted in Scheme 2). Such a charge distribution was indicated before for tetraphenylhexaazaanthracene[40] (**4a**) by Wudl, Houk, and co-workers.[25]

The ΔE_{ST} values for the studied TPH-anthracenes are generally smaller than those of the related TPH-acridines (Table 4). As the TPH-acridines generally display dipole moments larger than those of TPH-anthracenes, these results might imply that the greater charge separation or the higher polarity, the larger the singlet−triplet energy splitting might be. To test this correlation, we studied the relationship between ΔE_{ST} and the total dipole moment for a wide range of molecules with various substituents. The large permanent dipole moments (the zwitterionic character) in this family of compounds make them promising candidates for field-based switching (Table 4).[41]

(33) (a) Strassner, Th.; Weitz, A.; Rose, J.; Wudl, F.; Houk, K. N. *Chem. Phys. Lett.* **2000**, *321*, 459. (b) Winkler, M.; Houk, K. N. *J. Am. Chem. Soc.* **2007**, *129*, 1805.
(34) Wolinski, K.; Hinton, J. F.; Pulay, P. *J. Am. Chem. Soc.* **1990**, *112*, 8251.
(35) (a) Ruiz-Morales, Y. *J. Phys. Chem. A* **2004**, *108*, 10873. (b) Chen, Z.; Wannere, C. S.; Corminboeuf, C.; Puchta, R.; Schleyer, P. v. R. *Chem. Rev.* **2005**, *105*, 3842.
(36) Keith, T. A.; Bader, R. F. W. *Chem. Phys. Lett.* **1993**, *210*, 223.
(37) Frisch, M. J. *Gaussian03*. The full reference can be found in the Supporting Information.
(38) (a) Norton, J. E.; Houk, K. N. *J. Am. Chem. Soc.* **2005**, *127*, 4162. (b) Bendikov, M.; Duong, H. M.; Starkey, K.; Houk, K. N.; Carter, E. A.; Wudl, F. *J. Am. Chem. Soc.* **2004**, *126*, 7416.
(39) (a) Kato, T.; Yamabe, T. *J. Phys. Chem. A* **2004**, *108*, 11223. (b) Kato, T.; Yamabe, T. *J. Phys. Chem. B* **2005**, *109*, 10620. (c) Kato, T.; Yamabe, T. *J. Phys. Chem. A* **2005**, *109*, 4804.
(40) Pierron, P. *Ann. Chim. Phys.* **1908**, *15*, 269.
(41) Gibbs, H. M. *Optical Bistability: Controlling Light with Light*; Academic Press: New York, 1985.

TABLE 4. B3LYP/6-31G(d,p) Computed Zero-Point Vibrational Energies [kcal mol^{-1}], Singlet-Triplet Energy Separations [kcal mol^{-1}], Difference of Total Dipole Moments ($\Delta\mu_{ge}$) [D] between Ground (μ_g) and Excited States (μ_e), HOMO−LUMO Energy Gaps [kcal mol^{-1}] and B3LYP/6-311G(d,p)//B3LYP/6-31G(d,p) λ_{max} [nm] of 3a−i, 4a, and 4b

				ZPVE							
No.	X	Ar^1	Ar^2	singlet	triplet	ΔE_{ST}[a]	μ_g	μ_e	$\Delta\mu_{ge}$	Δ_{HL}	λ_{max}
3a	N	Ph	Ph	286.1	292.5	−20.8	8.19	7.07	1.12	57.7	513
3b	N	Ph	*p*-$CH_3C_6H_4$	320.4	319.4	−21.0	9.28	8.21	1.07	57.7	513
3c	N	*p*-$CH_3C_6H_4$	Ph	320.4	292.6	−20.7	7.53	6.37	1.16	57.4	518
3d	N	*p*-ClC_6H_4	Ph	273.9	272.9	−21.0	10.68	9.54	1.14	57.8	514
3e	N	*p*-ClC_6H_4	*p*-$CH_3C_6H_4$	308.2	307.2	−21.1	11.83	10.74	1.09	57.9	514
3f	N	*p*-$NO_2C_6H_4$	Ph	289.2	288.1	−21.5	14.69	13.52	1.17	58.4	552
3g	N	*p*-$NO_2C_6H_4$	*p*-$CH_3C_6H_4$	323.5	322.5	−21.6	15.91	14.80	1.11	58.3	558
3h	N	naphth-2-yl	Ph	344.8	343.7	−21.2	7.92	6.67	1.25	57.7	523
3i	N	pyrid-4-yl	Ph	271.2	270.2	−21.0	12.94	11.80	1.14	58.1	510
4a	C	Ph	Ph	293.5	292.6	−16.3	6.49	5.04	1.45	52.8	561
4b	C	*p*-$CH_3C_6H_4$	Ph	327.8	292.5	−16.2	5.91	4.42	1.49	52.7	562

[a] Negative value indicates a ground state singlet.

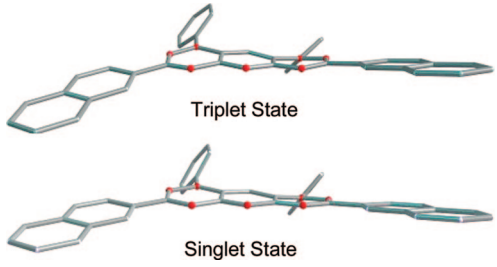

FIGURE 8. Similarity of the B3LYP/6-31G(d,p) optimized geometries of **3h** in the singlet and triplet states.

All structures show slightly twisted topologies and generally very small geometric differences between their singlet and triplet states (see **3h** with the most pronounced distortion, Figure 8). The rather similar geometries between singlet and triplet optimized structures lend credibility to the small ΔE_{ST} values. The twisting angles $\varphi(N^1C^{14}C^8N^7)$ of the fused moiety in the TPH-acridines are more pronounced than those in TPH-anthracenes (see Supporting Information), which is in line with the larger ΔE_{ST} and the greater zwitterionic character. The distortion must be due to the steric demand of the aryl groups in the *peri*-positions. The structures of the hexaazaanthracene and hexaazaacridine moieties (without the aryl groups) are both coplanar with $\varphi(N^1C^{14}C^8N^7) = 0.0°$ at the same level of theory. In phenyl-substituted structures, the aryl rings are connected by C−C (Ar^1, Figure 6) and C−N bonds (Ar^2) to two different positions of the fused moiety.

As shown in Figure 8, the steric repulsion of the Ar^2's in the *peri*-positions and also the nature of the C−N bonds twist these rings (Ar^2's) noticeably more away from the plane of the fused moiety than those joined through CC bonds (Ar^1's). The variation of the dihedral angles $\varphi(C^{16}C^{15}C^{14}N^{13})$ for the Ar^1 and $\varphi(C^{18}C^{17}N^2C^3)$ for the Ar^2 in the singlet and triplet states provides an explanation for the different degrees of π-delocalization in these overall nonplanar molecules. The X-ray structure of **3g** shows no twisted topology in the fused moiety, which we attribute to packing effects.

As discussed above, pronounced bathochromism, depending on the polarity of the solvent, was observed for all TPH-acridines **3a**−**i** and for TPH-anthracenes **4a**,**b**. Following Clar's ideas,[42] only one aromatic sextet can exist in linear oligoacenes and by extension also in their aza analogues. With an infinite number of rings, these systems become cyclic polyenes in which one aromatic sextet is not enough to provide a sufficient degree of stability.[42] Repeated benzannulation increases their reactivity and produces the observed bathochromic shifts. Clar was the first to notice that the more intensively colored a benzenoid hydrocarbon is, the less stable it generally is. He ascribed this relationship to a bathochromic shift of the p-band as the stability decreases.[42] A similar bathochromism was observed for substituted twistacenes;[38a,43] linear polyacenes are characterized by remarkably large shifts in their UV p-bands.

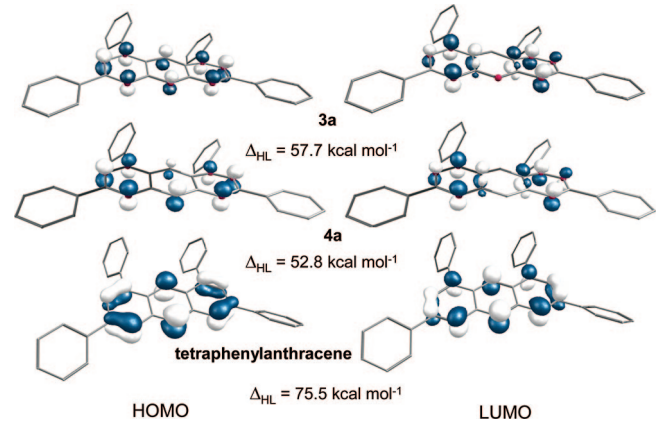

FIGURE 9. The B3LYP/6-31G(d,p) frontier molecular orbitals for TPH-acridine (**3a**), TPH-anthracene (**4a**), and tetraphenylanthracene (TP-anthracene).

For a better understanding of the UV-vis spectra, we computed these with TD-DFT. Low transition energies (long wavelengths) imply a small HOMO−LUMO energy gap (Δ_{HL}) that frequently results in high reactivity;[44] computed λ_{max} values as well as Δ_{HL} are presented in Table 4. The bathochromic shifts are a result of the degree of p/π-delocalization that is also affected by the substituents. The nature of the *para*-substituents (A^1 and A^2 in Figure 6) and the position (Ar^1 and Ar^2) both affect λ_{max}. The λ_{max} values of the TPH-anthracenes are generally larger than those of TPH-acridines. For example, the λ_{max} of unsubstituted TPH-anthracene (**4a**) is 561 nm and of unsubstituted TPH-acridine (**3a**) it is 513 nm.

The TPH-acridine and TPH-anthracene frontier orbitals, which display significant antibonding character, are considerably

(42) Clar, E. *The Aromatic Sextet*; Wiley: London, 1972.

(43) (a) Duong, H. M.; Bendikov, M.; Steiger, D.; Zhang, Q.; Sonmez, G.; Yamada, J.; Wudl, F. *Org. Lett.* **2003**, *5*, 4433. (b) Notario, R.; Abboud, J.-L. M *J. Phys. Chem. A* **1998**, *102*, 5290.

(44) Wiberg, K. B. *J. Org. Chem.* **1997**, *62*, 5720.

TABLE 5. B3LYP/6-311G(d,p)//B3LYP/6-31G(d,p) Total NICS Values Related to the Ring Center for 3a−i, 4a, and 4b (in ppm)

NICS	3a	3b	3c	3d	3e	3f	3g	3h	3i	4a	4b
0.0 (inner ring)	+0.2	+0.2	+0.1	+0.1	+0.1	+0.4	+0.5	−0.9	+0.2	−2.1	−2.3
0.0 (outer rings)	+1.6	+1.6	+1.4	+1.3	+1.5	+2.0	+1.9	+0.5	+1.7	+2.9	+3.1
1.0 (inner ring)	−2.9	−2.9	−3.1	−3.1	−3.2	−2.7	−2.8	−3.5	−2.9	−4.7	−4.7
1.0 (outer rings)	−1.8	−1.8	−1.7	−1.6	−1.7	−1.5	−1.5	−1.4	−1.7	−0.2	−0.8

different from those of tetraphenylanthracene (Figure 9). In TPH-acridines and TPH-anthracenes, the frontier orbitals have large amplitudes on the fused moieties that are centered on the nitrogen atoms and no coefficients on the two terminal carbon atoms bonded to phenyl substituents. The HOMO has large coefficients on the electronegative nitrogen atoms; this diminishes the antibonding character in nitrogen-rich TPH-acridines relative to their TPH-anthracene analogues. As a consequence, the experimental and computed HOMO−LUMO gaps for TPH-acridines are larger, which is in agreement with a smaller λ_{max}. Carbon-bonded electron-donating and electron-withdrawing groups (position A[1], Figure 6) cause smaller and larger Δ_{HL} and ΔE_{ST}, respectively (Table 4). Hence, from a conceptual viewpoint, TPH-anthracene derivatives are more attractive targets to achieve stable organic structures with small ΔE_{ST} values.

3. Magnetic Properties. ^{13}C chemical shifts and nucleus-independent chemical shielding (NICS) DFT computations provide additional information to understand the electronic structures of the present systems. The GIAO-computed ^{13}C and ^{1}H NMR chemical shifts generally agree well with experimental data (see Supporting Information). The average deviation of the computed δ ^{1}H and δ ^{13}C shifts relative to experimental data is about 1.4 and 8.0 ppm, due to the neglect of solvent effects in the NMR computations.

Delocalization effects were evaluated by computing NICS(0) as well as NICS(1) values (Table 5). As references, the NICS values for benzene, 1,2,4-triazine, cyclobutadiene, and the related aliphatic ring structures shown in Figure 10 were computed at the same level of theory.

The NICS data of the synthesized structures were compared to reference structures depicted in Figure 11. As noted before, the NICS values at the ring centers indicate weak antiaromaticity for **3a** in all core rings, but the antiaromatic character vanishes quickly above the planes of the rings (NICS = 1.0 Å). Nevertheless, ring currents play a very minor role as the absolute magnitudes of the NICS values are rather small. Indeed, the values are close to those of fully saturated 1,2,4-triazinane, which is considered nonaromatic (Figure 10). The aromatic counterpart 1,2,4-triazine is clearly defined as such by its large negative NICS values. A comparison with the ΔE_{ST} values shows that there is no obvious relationship between these two quantities. If anything, a small ΔE_{ST} in a cyclic delocalized structure manifests itself by a small absolute NICS(0) value.

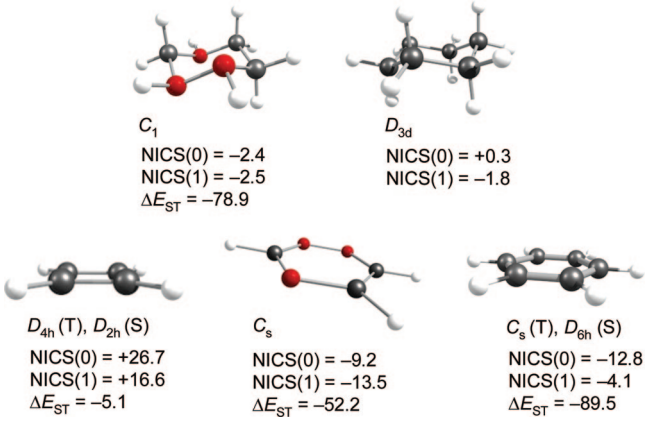

FIGURE 10. B3LYP/6−311G(d,p)//B3LYP/6−31G(d,p) NICS(0) and NICS(1) values (ppm) and ΔE_{ST} (kcal/mol) for benzene, cyclobutadiene (the NICS values are for singlet state), and related structures as reference systems. The ΔE_{ST} is not available for cyclohexane because of dissociation upon optimization in the triplet state.

4. Substituent Effects. For a comprehensive comparison, we studied a number of substituted hexaazaacridine and hexaazaanthracene derivatives to determine the role of the substituents on the ΔE_{ST} values. To maximize the effect, we first investigated structures with substituents bonded directly to the N or C atoms of the fused moieties without using the phenyl groups. The structural configurations are shown in Figure 12.

A large variety of substituents Y (Figure 12) with a broad spectrum of mesomeric and inductive effects were employed. Halogens showed dissociation of the N−Hal bond (weakly bound complexes form) in their optimized triplet state structures in configurations **i** and **ii**, and these results are not discussed. Our data demonstrate that the electronic properties, the number, and the position of the substituents have a large effect on the ΔE_{ST} values in these molecules (Figure 13).

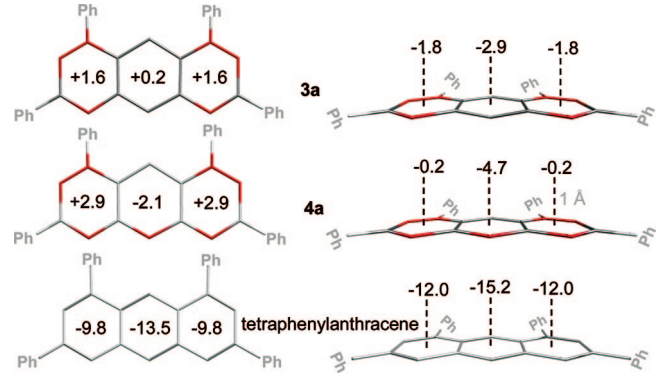

FIGURE 11. B3LYP/6-311G(d,p)//B3LYP/6−31G(d,p) computed NICS(0) and NICS(1) values for TPH-acridine (**3a**), TPH-anthracene (**4a**), and TP-anthracene.

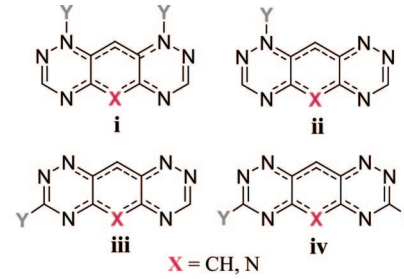

Y = Li, OCH_3, CH_3, NMe_2, NH_2, H, SiH_3, CF_3, CCl_3, CBr_3, $C(O)CH_3$, CN, C(O)H, NO_2, C(O)Cl, BH_2, F, Cl, Br

FIGURE 12. Model systems to study the substituent effects on the electronic structures of hexaazaacridine as well as hexaazaanthracene derivatives.

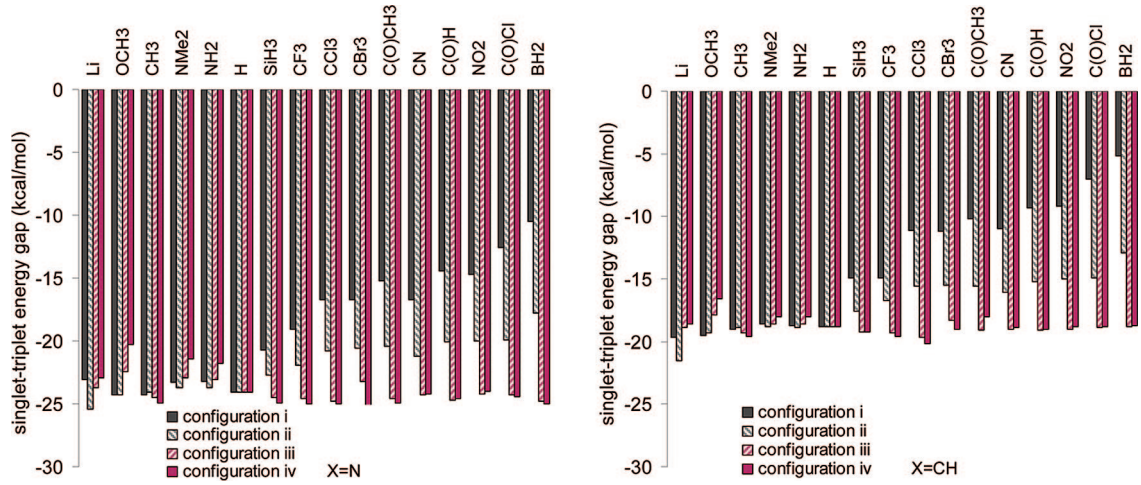

FIGURE 13. Relative changes of B3LYP/6-31G(d,p) ΔE_{ST} values (kcal mol^{-1}) depending on the substituents for hexaazaacridine (X = N, left) and hexaazaanthracene (X = CH, right) derivatives.

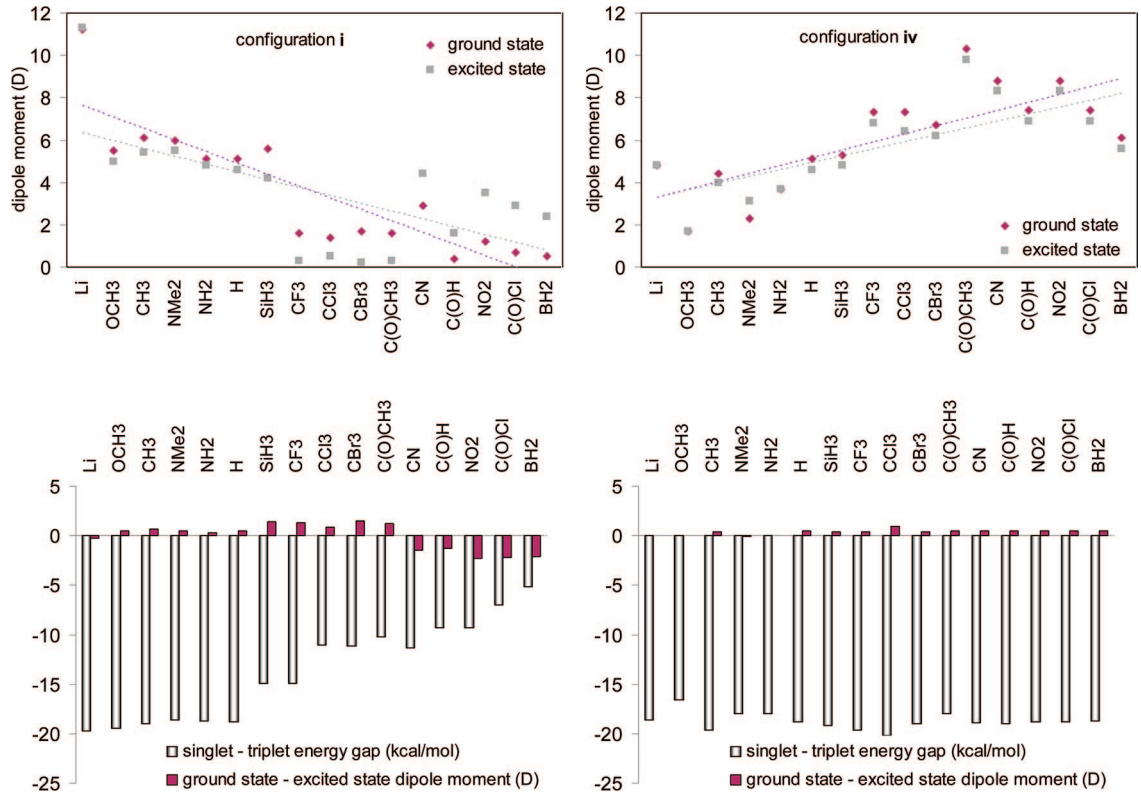

FIGURE 14. Comparing the trends in changes of the total dipole moments due to the two different structural configurations **i** (left) and **iv** (right) for substituted hexaazaanthracene derivatives in ground and first excited states (top). The lines should make the trends of the $\Delta\mu_{ge}$ values more visible. The correlation between ΔE_{ST} values (kcal mol^{-1}) and $\Delta\mu_{ge}$'s (D) for these systems (bottom). All data were obtained at B3LYP/6-31G(d,p).

Configurations **i** and **ii** with N-substitution in the *peri*-position(s) are more susceptible to electronic effects than **iii** and **iv**, which are substituted at carbon (Figures 12 and 13). This can be understood on the basis that the carbons bearing the substituents are incapable of proper π-conjugation (see MO renderings in Figure 9). The nitrogen atom at the *peri*-position *is* part of the conjugated system of the fused ring moieties, and as a result, substituents at this position show relatively large effects (configurations **i** and **ii**). The number of the substituents is also important: The changes of ΔE_{ST} values in **i** are larger than those in **ii**. These effects are attenuated with the C-bonded substituents in **iii** and **iv**.

As noted above, the ΔE_{ST} values of hexaazaanthracenes (X = CH) are smaller than those of the analogous hexaazaacridines (X = N). The main reason for this finding is the lower polarity (smaller zwitterionic character) of the hexaazaanthracenes (the total dipole moment for parent hexazaanthracene is 6.49 and 8.19 D for hexaazaacridine in their ground states). A comparison between the computed total dipole moments and the ΔE_{ST} values confirms that generally as the total dipole moment of a molecule decreases the ΔE_{ST} increases (Figures 14; however, compare discussion above). The total dipole moments decrease more rapidly in system **i** than in **ii**. The same correlation is found for **iii** and **iv**. For all four studied configurations, the changes of

TABLE 6. Rationalization of Inductive Substituent Effect on the ΔE_{ST} (kcal mol^{-1}) B3LYP/6-31G(d,p) for Hexaazaanthracene Derivatives (configuration i)[a] [ISE = Inductive Substituent Effect (±I)]

Y	−Li[b]	−OCH_3	−CH_3	−NMe_2	−NH_2	−H	−SiH_3	−CF_3
ΔE_{ST}	−19.7	−19.5	−19.0	−18.7	−18.7	−18.8	−14.9	−14.9
Δq_C^{11} (NBO)[c]	−0.011	−0.002	−0.003	−0.001	+0.002	±0.000	+0.004	+0.011
ISE	−I	−I	−I	−I	+I	−	+I	+I
Y	−CCl_3	−CBr_3	−C(O)CH_3	−CN	−C(O)H	−NO_2	−C(O)Cl	−BH_2
ΔE_{ST}	−11.1	−11.2	−10.2	−11.3	−9.3	−9.3	−7.0	−5.2
Δq_C^{11} (NBO)[c]	+0.012	+0.013	+0.015	+0.025	+0.017	+0.019	+0.023	+0.052
ISE	+I	+I	+I	+I	+I	+I	+I	+I

[a] Negative value indicates that the singlet state is more stable. [b] Li displays η^2-coordination upon optimization. [c] Relative local natural charge on carbon atom *meso*-C^{11} in Figure 6 ISE relative to −H; the natural charge for −H is −0.315.

the dipole moments are more irregular than the changes of the ΔE_{ST} values.

The influence of the relative magnitudes of the dipole moments of the ground and first excited states ($\Delta\mu_{ge} = \mu_g - \mu_e$) on the singlet−triplet energy gaps was also studied. For nitrogen-substituted structures (**i** and **ii**), the amount of $\Delta\mu_{ge}$ and the changes promoted by the substituents are more noticeable than that in the carbon-substituted structures (**iii** and **iv**). It could be speculated that the greater the dipole moment of the excited state is relative to the ground state, the more the singlet−triplet energy gap increases; however, some hexaazaacridine structures (X = N) show irregularities. Tables containing μ_g, μ_e, and $\Delta\mu_{ge}$ for all configurations and the figures presenting these correlations for hexaazaanthracenes and hexaazaacridines are available in the Supporting Information.

The relative energies of the singlet and triplet states of molecules with structures **i** and **ii** (Y bonded to a nitrogen atom) show that generally the introduction of deactivating groups (EWG) strongly favors the triplet state. Electron-donating groups (EDG) such as −OCH_3, −NMe_2, and −NH_2 destabilize preferentially the triplet relative to the singlet state. For example, the ΔE_{ST} values for the hexaazaanthracenes (configuration **i**) with −OCH_3, −NH_2, −CN, and −NO_2 substitutions are −19.5, −18.7, −11.3, and −9.3 kcal mol^{-1}, respectively. The structural configurations **iii** and **iv** (Y bonded to a carbon atom) are generally not sensible enough to substituent effects. For a rationalization of the substituent-induced changes of the ΔE_{ST} values, in the following, the results based on the configuration **i** with *meso*-carbon atom (X = CH) as the most sensitive system are presented (the data for other systems are available in the Supporting Information).

I. Inductive Substituent Effects. We compared the ΔE_{ST} values with the relative amount of intramolecular charge transfer caused by the various substituents by examining the local natural electron populations (NPAs) on the carbon atom *meso*-C^{11} (X = CH) in structure **i** for which these effects should be most apparent.[45,46] Similarly, Komorowski et al. as well as Geerlings et al. described substituent effects by means of reactivity indices such as group hardness and group electronegativity.[47] The relative intramolecular charge transfer (Δq_C) due to the inductive substituent effect relative to −H shows that as Δq_C on *meso*-C,[11] the singlet−triplet energy gaps decrease (Table 6). As a result, N-bonded σ-acceptor substituent groups decrease the ΔE_{ST}.

The same strategy was followed for *meso*-C^{11} (X = CH) in structure **iv** with different carbon-bonded substituents. A mild inverse effect with some irregularities is observed. The most positive ISE is obtained by using −Li (+0.20), −NMe_2 (+0.015), and −NH_2 (+0.013) and the most negative ISE observed for −NO_2 (−0.018), −C(O)Cl (−0.016), and −CBr_3 (−0.014) relative to −H. The corresponding table is presented in the Supporting Information.

II. Mesomeric Substituent Effects. Mesomeric substituent effects (±M) mainly concern resonance (delocalization) effects. Aromaticity and hence cyclic delocalization indices typically rely on three common (but not exclusive) features: increased thermodynamic stability, decreased bond length alternation, and characteristic magnetic properties.[32] In the present work, we analyze the ± M effects of the substituents and their influence on the π-electron system using the NICS aromaticity criteria.

First of all, there is no direct correlation between the computed NICS(1) values and the ΔE_{ST} values. For the more useful $NICS_{zz}(1)$ criteria, introduced by Schleyer et al. as a better measure for the π-delocalization,[48] a correlation is more apparent (Figure 15).

In structure **i**, the computed $NICS_{zz}(1)$ values show that the outer rings of all structures are antiaromatic with $NICS_{zz}(1)$ between +7 and +18. For comparison, the $NICS_{zz}(1)$ values for benzene are −29.11 and +57.81 for cyclobutadiene (C_{2h}, singlet) at the same level of theory. Comparison of the values shows a decrease of the $NICS_{zz}(1)$ in both the inner rings and the outer rings with growing ΔE_{ST} values; this effect is more apparent in the inner ring than in the outer rings. As a result, in structure **i**, π-acceptors (−M substituents) increase the aromatic character of the inner ring while π-donors (+M substituents) destabilize the system by increasing the electron density of the outer rings.

Owing to the MO pattern of configuration **iv**, no regular relationship could be identified between ΔE_{ST} values and the $NICS_{zz}(1)$ values. As a result, carbon-bonded substituents have only very little effect on the ΔE_{ST} values. This is in agreement with our analyses of the experimentally prepared derivatives above.

Next we studied the effects of *push*−*pull* substitution, using a fixed NO_2 group as an ideal ΔE_{ST}-lowering reference substituent (−I and −M effects) in the N-position of hexaazaanthracene (**I**−**IV**, Figure 16). The computed ΔE_{ST} values of these structures with varying the substituents are presented in Figure 17.

Generally the ΔE_{ST} values are smaller in these four configurations compared to the related systems **i**−**iv**; the average

(45) (a) Wiberg, K. B. *Acc. Chem. Res.* **1999**, *32*, 922. (b) Perez, P.; Toro-Labbe, A.; Contreras, R. *J. Phys. Chem. A* **2000**, *104*, 5882.
(46) Bailey, P.; Ashton, J. *J. Org. Chem.* **1957**, *22*, 98.
(47) (a) Komorowski, L.; Lipinski, J.; Pyka, M. J. *J. Phys. Chem.* **1993**, *97*, 3166. (b) Proft, F. D.; Langenaeker, W.; Geerlings, P. *J. Phys. Chem.* **1993**, *97*, 1826. (c) Proft, F. D.; Amira, S.; Choho, K.; Geerlings, P. *J. Phys. Chem.* **1994**, *98*, 5227.
(48) Corminboeuf, C.; Heine, T.; Seifert, G.; Schleyer, P. v. R.; Weber, J *Phys. Chem. Chem. Phys.* **2004**, *6*, 273.

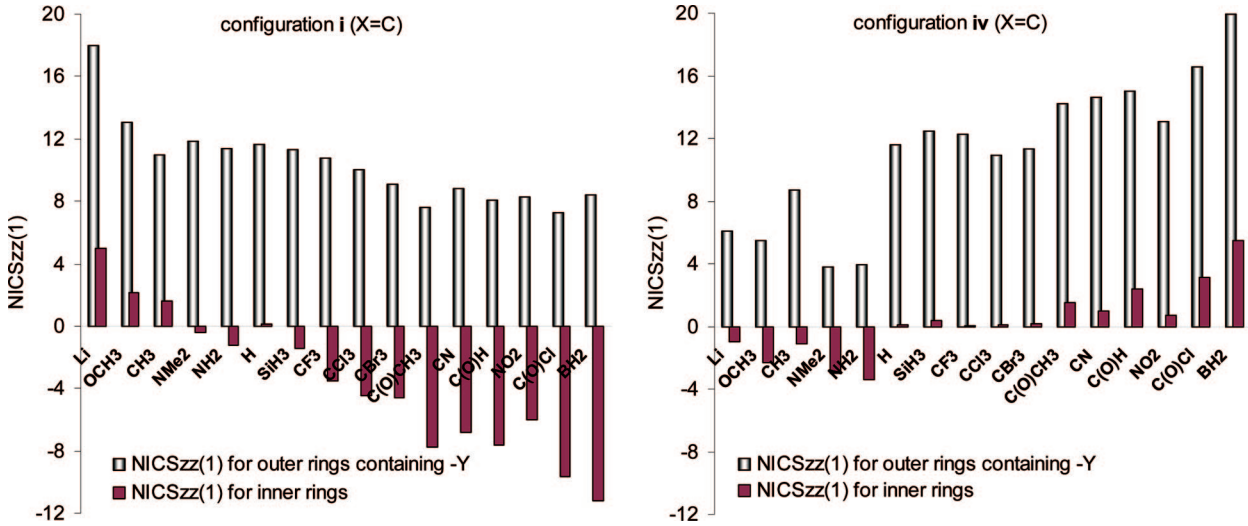

FIGURE 15. Trends in $NICS_{zz}(1)$ at B3LYP/6-311G(d,p)//B3LYP/6-31G(d,p) in substituted hexaazaanthracene derivatives with configurations **i** (substituents with strong positive resonance effect cause smaller ΔE_{ST} values) and **iv** (the resonance effect shows no regular influence on ΔE_{ST} values).

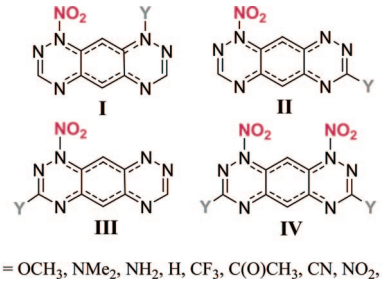

Y = OCH_3, NMe_2, NH_2, H, CF_3, $C(O)CH_3$, CN, NO_2, BH_2

FIGURE 16. Push−pull systems with fixed σ- and π-acceptor NO_2 substituent(s).

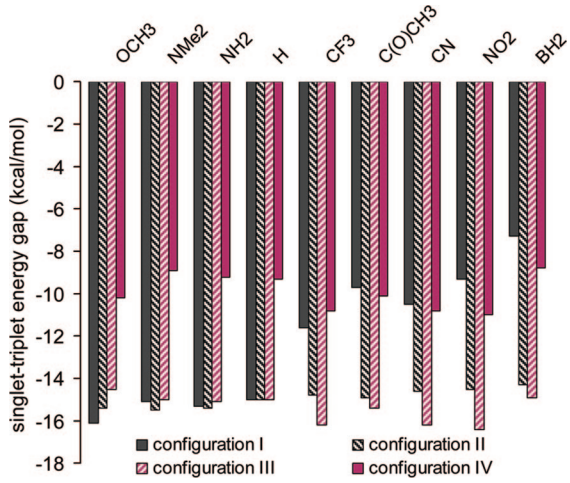

FIGURE 17. Trends of ΔE_{ST} values in substituted hexaazaanthracene derivatives with push−pull structural configurations **I**−**IV**.

reduction is ca. 4 kcal mol^{-1} for **I**−**III**/**i**−**iii** and ca. 8 kcal mol^{-1} for **IV**/**iv**. The noticeable reduction for structure **IV** can be explained by having two N-bonded NO_2 substituents. The structural configuration **IV** containing nitrogen-bonded substituents with both −I and −M effects and carbon-bonded substituents with a +I effect is suggested to be the optimum combination to affect the electronic structure for hexaazaanthracene to provide a small ΔE_{ST}. Structure **I** is also presented as the second favorable configuration with two N-bonded σ- and π-acceptor substituents (Figure 17).

5. Extension of π-Delocalization. Finally, we investigated the effect of extending the π-delocalization when *p*-phenyl groups are placed between the central moiety and the substituents (as in most of the experimentally available systems). While this has little effect on reducing the ΔE_{ST} values when the phenyl groups are bonded to carbon, the ΔE_{ST} values are reduced for N-bonded phenyl substituents (Figure 21).

With *p*-substituted phenyl groups as spacers, the ΔE_{ST} values are generally less sensitive to substituent effects (Table 7). This attenuation of the substituent effects can be attributed to some twisting of the two phenyl groups (Ar^2 in Figure 6) that causes loss of overlap. Hence, the ΔE_{ST} values decrease most significantly when strongly π-delocalized, electron-withdrawing groups bonded to the nitrogen positions are used; electron-donating groups attached to carbon only cause a mild reduction of the ΔE_{ST} values (Figure 22).

Conclusions

A variety of novel tetraphenylhexaazaacridines and tetraphenylhexaazaanthracenes were synthesized and fully characterized. These structures are promising candidates for purely organic materials with very low-lying singlet−triplet energy separations. The pronounced bathochromism and the appearance of the fluorescence spectra as well as a comparison with computed natural charges identify these compounds as zwitterionic singlet ground state molecules with rather low-lying triplet states.

A comprehensive experimental and DFT investigation of the electronic properties of azaacridines and azaanthracenes reveals several important clues for understanding the electronic structures of these molecules. Generally, TPH-anthracenes show ΔE_{ST} values smaller than those of TPH-acridines. The larger ΔE_{ST} of the latter is in line with their somewhat more twisted topology, greater total dipole moment (more zwitterionic character), greater dipole moment of the first excited state relative to the ground state, and a larger λ_{max} in the UV absorption spectra.

A systematic computational analysis reveals that the electronic properties, the number, and the position of a series of substituents have a large effect on the ΔE_{ST} values (Figure 20). Nitrogen-bonded substituents show larger effects than those

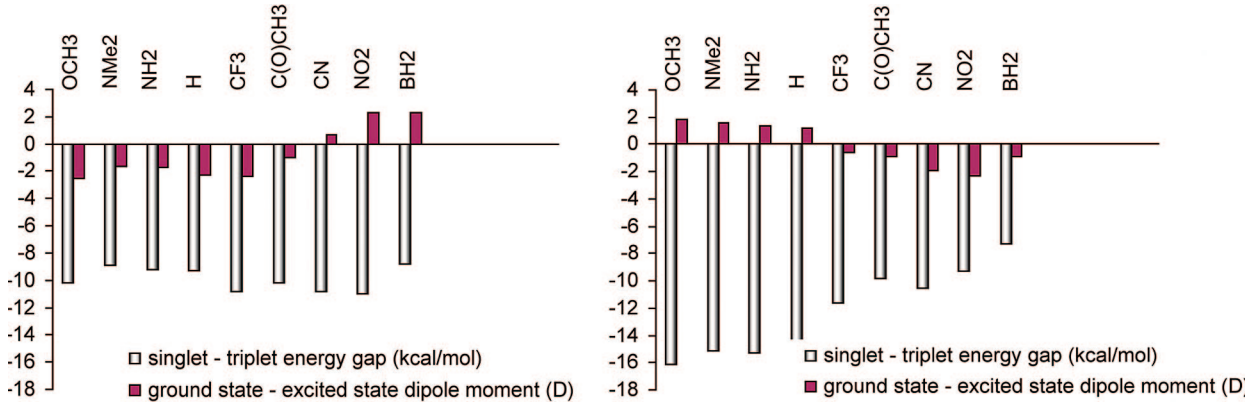

FIGURE 18. The correlation between ΔE_{ST} values (kcal mol^{-1}) and $\Delta\mu_{ge}$ values (D) for two structural configurations **I** (right) and **IV** (left) for substituted hexaazaanthracenes. All data were obtained at B3LYP/6-31G(d,p).

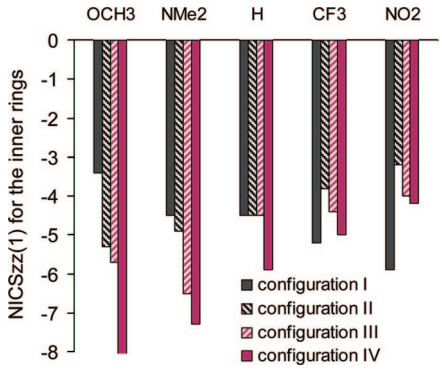

FIGURE 19. Trends of NICS$_{zz}$(1) for the inner rings of selected substituted hexaazaanthracene derivatives with configuration **I**−**IV** at the B3LYP/6-311G(d,p)//B3LYP/6-31G(d,p) level of theory.

bonded to carbon, owing to the general molecular orbital structure of these systems that favors the involvement of π-delocalization via the nitrogen atoms. The ΔE_{ST} values in N-bonded pull−pull electronic systems are smaller than in pull−push and push−push systems. For TPH-anthracene, this reduction is as large as −8.9 kcal mol^{-1} compared to the unsubstituted parent system with a ΔE_{ST} of −18.8 kcal mol^{-1}. We are currently engaged in the design of new azaacenes with respect to optimizing π-electron delocalization and also functionalizing other heteroacenes to minimize the ΔE_{ST} values or to obtain triplet ground state structures.

Experimental Section

General Comments. All solvents were dried by standard methods, and all reactions were carried out under an inert atmosphere. For ^{1}H and ^{13}C NMR spectra, the deuterated solvents indicated were used. Mass spectrometric data (MS) were obtained by electron ionization (EI, 70 eV), chemical ionization (CI, H_2O), or electrospray ionization (ESI). For preparative scale chromatography, silica gel (60−200 mesh) was used. Melting points are uncorrected.

***N,N′*-Di(benzoyl)-2,6-diaminopyridine (6a).** To an ice-cold suspension of 2,6-diaminopyridine (5.50 g, 50.0 mmol) and NEt_3 (10.10 g, 100.0 mmol) in dry dichloromethane (150 mL) was added dropwise a dichloromethane solution (50 mL) of benzoyl chloride (14.06 g, 100.0 mmol). The reaction mixture was stirred at 20 °C for 12 h and subsequently poured into 200 mL of water. The organic layer was separated, washed with an aqueous solution of $NaHCO_3$ (200 mL, 5%) and with water, and dried ($MgSO_4$). The solution was filtered and concentrated under reduced pressure, and the residue was recrystallized from ethanol: Yield 7.60 g (48%), colorless prisms (ethanol), mp 177−179 °C; IR (KBr) $\tilde{\nu}$ = 3340 (s), 3061, 3035, 3006 (w), 1653, 1586, 1526, 1487, 1459 (s), 1396 (m), 1307 (s), 1269, 1242 (m), 1189, 1161, 1128, 1078, 903 (w),

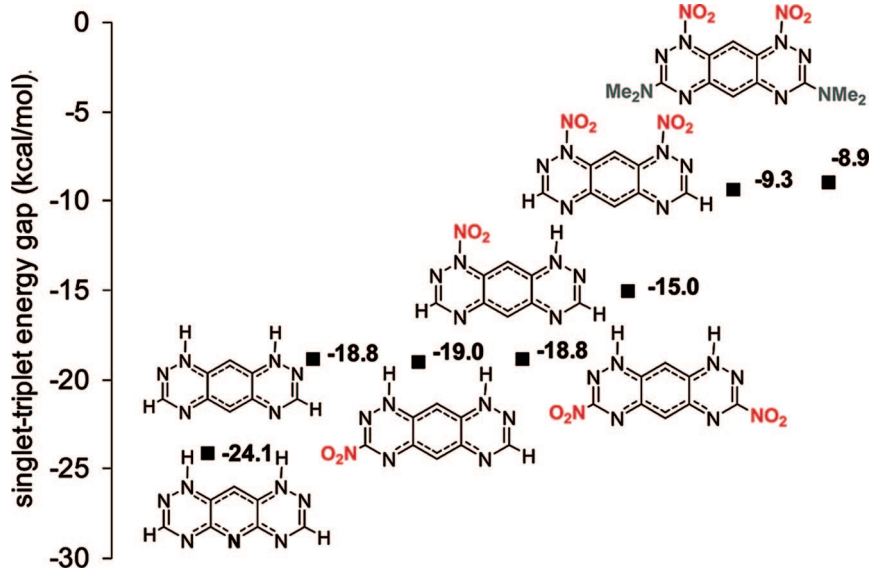

FIGURE 20. Trend of reduction in ΔE_{ST} values through improving the structural configurations.

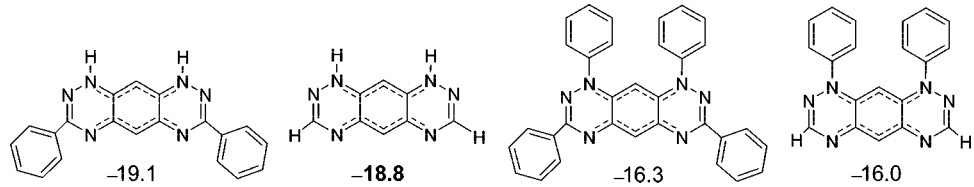

FIGURE 21. The effect of π-delocalization extension on reduction of the ΔE_{ST} value (kcal mol^{-1}).

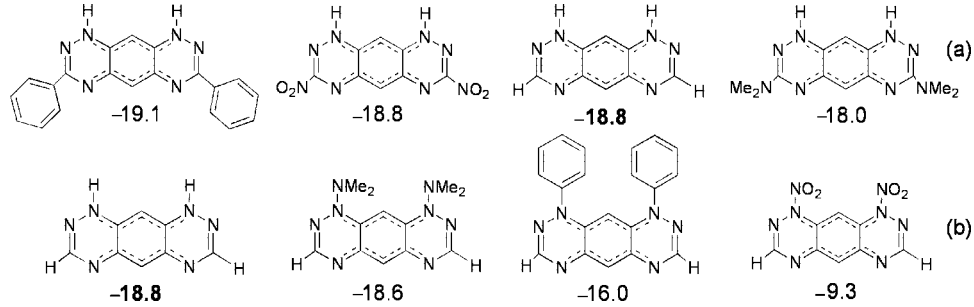

FIGURE 22. Comparison of the π-delocalization and substituent effects on the reduction of the ΔE_{ST} values (kcal/mol^{-1}) in carbon-bonded (a) and nitrogen-bonded (b) systems, separately.

TABLE 7. Comparison of the Substituent Effect on ΔE_{ST} Values (kcal mol^{-1}) with and without Using Phenyl Spacers

X	Ar^1	Ar^2	ΔE_{ST}
N	Ph/H	Ph/H	−20.8/−24.1
CH	Ph/H	Ph/H	−16.3/−18.8
CH	Ph/H	*p*-$NMe_2C_6H_4/NMe_2$	−17.0/−18.6
CH	Ph/H	*p*-$NO_2C_6H_4/NO_2$	−14.1/−9.3
CH	*p*-$NMe_2C_6H_4/NMe_2$	Ph/H	−15.8/−18.0
CH	*p*-$NO_2C_6H_4/NO_2$	Ph/H	−16.8/−18.8
CH	*p*-$NMe_2C_6H_4/NMe_2$	*p*-$NO_2C_6H_4/NO_2$	−13.2/−8.9

796, 710, 690, 632 (s), 582 (w); ^{1}H NMR ($CDCl_3$, 300 MHz) δ = 7.47−7.60 (m, 6 H, Ar), 7.81 (t, J = 8.1 Hz, 1 H, H-4, Pyr), 7.88−7.92 (m, 4 H, Ar), 8.11 (d, J = 8.1 Hz, 2 H, H-3, H-4, Pyr), 8.33 (br s, 2 H, NH); ^{1}H NMR (DMSO-d_6, 300 MHz) δ = 7.50−7.61 (m, 6 H), 7.91−8.40 (m, 7 H), 10.50 (s, 2 H); ^{13}C NMR (DMSO-d_6, 75 MHz) δ = 111.2, 127.8, 128.3, 131.9, 133.9, 139.8, 150.4, 165.7; MS (EI, 70 eV) *m*/*z* (%) = 318 (12, $[M + H]^+$), 317 (72, $[M]^+$), 290 (11), 289 (85), 288 (100), 221 (11), 105 (37). Anal. Calcd for $C_{19}H_{15}N_3O_2$ (317.12): C, 71.94; H, 4.73; N, 13.25. Found: C, 72.26; H, 5.09; N, 13.47.

***N*,*N*′-Bis(4-methylbenzoyl)-2,6-diaminopyridine (6b).** The reaction was carried out following the procedure as given for the synthesis of **6a**, starting with *p*-methylbenzoyl chloride (15.50 g, 100.0 mmol), 2,6-diaminopyridine (5.50 g, 50.0 mmol), and NEt_3 (10.10 g, 100.0 mmol) in 200 mL of dichloromethane: Yield 10.70 g (62%), colorless prisms (ethanol), mp 215−217 °C; IR (KBr) $\tilde{\nu}$ = 3423 (m), 3344 (m), 3028, 2919 (w), 1653 (s), 1609 (m), 1584, 1529, 1497, 1456, 1302 (s), 1242, 796, 744, 616 (m); ^{1}H NMR (DMSO-d_6, 300 MHz) δ = 2.39 (s, 6 H), 7.32−7.35 (m, 4 H), 7.87−7.95 (m, 7 H), 10.36 (s, 2 H); ^{13}C NMR (DMSO-d_6, 150 MHz) δ = 21.0, 111.0, 127.9, 129.0, 131.2, 139.9, 142.1, 150.5, 165.5; MS (EI, 70 eV) *m*/*z* (%) = 346 (10, $[M + H]^+$), 345 (48, $[M]^+$), 317 (17), 316 (12), 119 (100), 91 (37). Anal. Calcd for $C_{21}H_{19}N_3O_2$ (345.40): C, 73.03; H, 5.54; N, 12.17. Found: C, 73.19; H, 5.25; N, 12.86.

***N*,*N*′-Bis(4-chlorobenzoyl)-2,6-diaminopyridine (6c).** The reaction was carried out following the procedure as given for the synthesis of **6a**, starting with 17.5 g of *p*-chlorobenzoyl chloride (100 mmol), 2,6-diaminopyridine (5.50 g, 50.0 mmol), and NEt_3 (10.10 g, 100.0 mmol) in 200 mL of dichloromethane. The solvent was removed under reduced pressure, the residue was suspended in 300 mL of water, and the suspension was stirred for 40 min. The solid was filtered off, suspended in 300 mL of an aqueous solution of $NaHCO_3$, and stirred for 40 min. The solid was filtered off, washed with water, and recrystallized from 2-propanol: Yield 10.40 g (54%), colorless prisms (2-propanol), mp 284 °C; IR (KBr) $\tilde{\nu}$ = 3424 (m), 3336 (s), 3094, 3062, 3041 (w), 1652, 1589, 1522, 1484, 1457, 1312 (s), 1243, 1093, 844, 797, 751, 634, 584, 542, 486 (m); ^{1}H NMR (DMSO-d_6, 300 MHz) δ = 7.59−7.62 (m, 4 H), 7.84−7.94 (m, 3 H), 8.01−8.04 (m, 4 H), 10.64 (s, 2 H); ^{13}C NMR (DMSO-d_6, 150 MHz) δ = 111.4, 128.5, 129.8, 132.8, 136.8, 140.0, 150.3, 164.8; MS (EI, 70 eV) *m*/*z* (%) = 387 (12, $[M]^+$, ^{37}Cl, ^{35}Cl), 385 (21, $[M]^+$, 2× ^{35}Cl), 357 (12), 141 (31), 139 (100), 112 (11), 110 (35). Anal. Calcd for $C_{19}H_{13}Cl_2N_3O_2$ (386.24): C, 59.09; H, 3.39; N, 10.88. Found: C, 58.73; H, 3.55; N, 10.85.

***N*,*N*′-Bis(4-nitrobenzoyl)-2,6-diaminopyridine (6d).** The reaction was carried out following the procedure as given for the synthesis of **6a**, starting with *p*-nitrobenzoyl chloride (18.56 g, 100.0 mmol), 2,6-diaminopyridine (5.50 g, 50.0 mmol), and NEt_3 (10.10 g, 100.0 mmol) in 200 mL of dichloromethane. The solvent was removed under reduced pressure, and the residue was suspended in 300 mL of water and refluxed for 40 min. The solid was filtered off, suspended in 300 mL of an aqueous solution of $NaHCO_3$, and stirred for 40 min. The solid was filtered off, washed with water, and refluxed in 2-propanol (150 mL) for 40 min: Yield 10.70 g (62%), colorless prisms, mp 270−274 °C; IR (KBr) $\tilde{\nu}$ = 3402, 3360, 3111 (w), 1694, 1658, 1602, 1585 (m), 1526, 1453, 1351 (s), 1301, 1250, 859, 715 (m); ^{1}H NMR (DMSO-d_6, 300 MHz) δ = 7.59−7.62 (m, 4 H), 7.84−7.94 (m, 3 H), 8.01−8.04 (m, 4 H), 10.64 (s, 2 H); ^{13}C NMR (DMSO-d_6, 600 MHz) δ = 111.9, 123.5, 129.5, 139.9, 140.3, 149.3, 150.2, 164.6; MS (EI, 70 eV) *m*/*z* (%) = 407 (34, $[M]^+$), 379 (19), 377 (24), 149 (100), 121 (38), 120 (55), 104 (51), 92 (28), 76 (25). $C_{19}H_{13}N_5O_6$ (407.34).

***N*,*N*′-Bis(naphth-2-oyl)-2,6-diaminopyridine (6e).** The reaction was carried out following the procedure as given for the synthesis of **6a**, starting with 2-naphthoylchloride (7.63 g, 40.0 mmol), 2,6-diaminopyridine (2.18 g, 20.0 mmol), and NEt_3 (4.05 g, 40.0 mmol) in 200 mL of dichloromethane. The solvent was removed under reduced pressure, and the residue was suspended in 300 mL of water and refluxed for 40 min. The solid was filtered off, suspended in 300 mL of an aqueous solution of $NaHCO_3$, and stirred for 40 min. The solid was filtered off, washed with water, and refluxed in 2-propanol (150 mL) for 40 min: Yield 5.82 g (70%), colorless prisms, mp 220−223 °C; IR (KBr) $\tilde{\nu}$ = 3340 (m), 3054 (w), 1653, 1588, 1515, 1454, 1307 (s), 1237, 801, 762 (m); ^{1}H NMR (DMSO-d_6, 300 MHz) δ = 7.65 (cm, 4 H), 7.96−8.10 (m, 11 H), 8.69 (m, 2 H), 10.67 (s, 2 H); ^{13}C NMR (DMSO-d_6, 600 MHz) δ = 111.1, 124.3, 126.8, 127.6, 128.0, 128.5, 129.1, 131.2, 132.0, 134.4, 140.0,

150.0, 165.8; MS (EI, 70 eV) *m/z* (%) = 419 (24, $[M + 2H]^+$), 155 (58, $[C_{10}H_7CO]^+$), 139 (14), 127 (41, $[C_{10}H_7]^+$). $C_{27}H_{19}N_3O_2$ (417.47).

***N,N′*-Bis(pyrid-4-oyl)-2,6-diaminopyridine (6f).** The reaction was carried out following the procedure as given for the synthesis of **6a**. *iso*-Nicotinoyl chloride (7.12 g, 40.0 mmol) was added at 0 °C to a suspension of 2,6-diaminopyridine (2.18 g, 20.0 mmol) and NEt_3 (8.10 g, 80.0 mmol) in dichloromethane (200 mL) over a period of 45 min. The solvent was removed under reduced pressure, and the residue was suspended in 300 mL of water and refluxed for 40 min. The solid was filtered off, suspended in 300 mL of an aqueous solution of $NaHCO_3$, and stirred for 40 min. The solid was filtered off, washed with water, and refluxed in 2-propanol (150 mL) for 40 min. The solid was filtered off and dried in vacuo: Yield 3.16 g (49%), colorless prisms, mp 275 °C (decomp); IR (KBr) $\tilde{\nu}$ = 3433 (m), 3145, 3043 (w), 1688, 1588 (s), 1554 (m), 1521 (s), 1490 (m), 1449 (s), 1413 (m), 1308 (s), 1243 (m), 803, 751, 699, 589 (w); ^{1}H NMR (DMSO-d_6, 300 MHz) δ = 7.88−7.99 (m, 7 H), 8.78−8.80 (m, 4 H), 10.90 (s, 2 H); ^{13}C NMR (DMSO-d_6, 600 MHz) δ = 111.9, 121.5, 140.2, 141.1, 150.1, 150.2, 164.6; MS (EI, 70 eV) *m/z* (%) = 319 (39, $[M]^+$), 291 (10), 290 (21), 241 (31), 105 (79), 79 (22), 78 (100). $C_{17}H_{13}N_5O_2$ (319.32).

***N,N′*-Bis(phenylimidoyl)-2,6-diaminopyridine dichloride (7a).** Bis(amide) **6a** (2.10 g, 6.6 mmol) and PCl_5 (4.01 g, 19.3 mmol) were suspended in dry toluene (20 mL). The mixture was stirred at 20 °C for 1.5 h and under reflux for 2 h. The solvent and $POCl_3$ were removed under reduced pressure. The residue was stored under argon at 4 °C to give a pale yellow solid: Yield 2.05 g (88%); ^{1}H NMR (300 MHz, $CDCl_3$) δ = 7.13 (d, *J* = 8.1 Hz, 2 H), 7.48−7.54 (m, 4 H), 7.60−7.66 (m, 2 H), 8.25 (t, *J* = 8.1 Hz, 1 H), 8.27−8.31 (m, 4 H); ^{13}C NMR (DMSO-d_6, 300 MHz) δ = 110.4, 128.1, 128.2, 128.5, 132.7, 132.7, 147.79, 167.1. MS (EI, 70 eV) *m/z* (%) = 355 (15, $[M]^+$, ^{37}Cl, ^{35}Cl), 353 (35, $[M]^+$, 2× ^{35}Cl), 320 (34), 318 (100, $[M - Cl]^+$ (^{35}Cl)), 217 (15), 215 (50), 179 (28), 89 (14), 77 (14); HRMS (EI, 70 eV) calcd for $C_{19}H_{13}N_3Cl_2$ 353.0486 ($[M]^+$, 2× ^{35}Cl), found *m/z* 353.0486 ± 2 ppm.

***N,N′*-2,6-(Pyridine)diylbis(benzamidrazone) (8a).** Bis(imidoyl) dichloride **7a** (2.10 g 6.0 mmol) was suspended in dry *n*-hexane (60 mL), and the mixture was cooled to 0 °C. To the mixture was dropwise added phenyl hydrazine (1.7 mL, 16.0 mmol). After stirring for 15 min, the ice bath was removed and the mixture was stirred at 20 °C for 14 h. The precipitated pale yellow solid was isolated by filtration and washed with *n*-hexane (30 mL): Yield 2.70 g (90%), colorless prisms; ^{1}H NMR (300 MHz, $CDCl_3$) δ = 6.80 (d, *J* = 7.8 Hz, 2 H), 7.50−7.38 (m, 7 H), 7.44−7.56 (m, 9 H), 7.83 (t, *J* = 7.8 Hz, 1 H), 8.19−8.22 (m, 4 H); MS (EI, 70 eV) *m/z* = 497 (M^+, 4), 480 (12), 91 (100). $C_{31}H_{27}N_7$ (497.60).

3,5,7,9-Tetraphenylhexaazaacridine (3a). To a well stirred solution of crude **8a** (2.50 g, 5.0 mmol) in methanol (120 mL) was dropwise added DBU (3.0 mL, 14.0 mmol). After stirring for a few minutes, the solution became dark red and a red-brownish solid began to precipitate. After stirring for 4 days, the solid was isolated by filtration and washed with 2-propanol. For purification, the solid was suspended in glacial acetic acid (10 mL) and stirred at 20 °C for 20 min. The red solid was isolated by filtration and washed with water and 2-propanol and dried in vacuo: Yield 0.742 g (30%), red solid; IR (KBr) $\tilde{\nu}$ = 3427 (m), 3059 (w), 1594 (m), 1503 (s), 1445 (s), 1396 (s), 1317 (s), 1171 (m), 1069 (m), 1006 (m), 859 (m), 777 (m), 699 (s), 634 (w); ^{1}H NMR (TFA-d_1, 600 MHz) δ = 5.75 (s, 1 H), 7.25−7.60 (m, 16 H), 7.95−8.15 (m, 4 H); ^{13}C NMR (TFA-d_1, 150 MHz) δ = 91.1, 126.3, 129.2, 131.2, 132.1, 132.5, 133.9, 135.4, 141.2, 141.5, 158.3, 158.6; UV−vis (AcOH) λ_{max} (log ϵ) = 273 (4.74), 535 (4.57) nm; UV−vis (DMF) λ_{max} (log ϵ) = 290 (4.76), 299 (4.74), 344 (3.81), 525 (4.50), 547 (4.51) nm; UV−vis (H_3PO_4) λ_{max} (log ϵ) = 540 (4.29) nm; UV−vis (H_2SO_4) λ_{max} (log ϵ) = 662 (4.34) nm; fluorescence (DMF) $F\lambda_{max}$ (λ_{Ex}) = 585 nm; MS (EI, 70 eV) *m/z* = 491 (M^+, 100), 77 (30); HRMS (EI, 70 eV) calcd for $C_{31}H_{21}N_7$ 491.1858 (M^+), found *m/z* 491.1858 ± 2 ppm.

Synthesis of 3a without Purification of the Intermediates. A suspension of **6a** (2.10 g, 6.6 mmol) and PCl_5 (4.01 g, 19.3 mmol) in dry toluene (40 mL) was stirred under reflux for 2 h. The solvent and $POCl_3$ were removed under reduced pressure to give **7a**. The residue (**7a**) was suspended in dry *n*-hexane (60 mL), the mixture was cooled to 0 °C, and phenyl hydrazine (1.7 mL, 16.0 mmol) was added under argon atmosphere. After a period of 15 min, the ice bath was removed and the mixture was stirred at 20 °C for 12 h. The pale yellow residue (**8a**) was filtered off, washed with *n*-hexane (30 mL), and dissolved in methanol (150 mL). To the well stirred suspension was dropwise added DBU (4.0 mL). After stirring for a few hours, the solution became dark red and a solid began to precipitate. After stirring for 5 days at 20 °C, the solid was filtered off and washed with 2-propanol. For purification, the solid was suspended in glacial acetic acid (10 mL) and stirred at 20 °C for 1.5 h. The red solid was isolated by filtration and washed with water and, subsequently, 2-propanol: Yield 0.742 g (23%), dark red solid.

5,7-Di(4-tolyl)-3,9-diphenylhexaazaacridine (3b). A suspension of **6a** (2.10 g, 6.6 mmol) and PCl_5 (4.01 g, 19.3 mmol) in dry toluene (20 mL) was stirred under reflux for 2 h. The solvent and $POCl_3$ were removed under reduced pressure to give **7a**. The residue (**7a**) was suspended in dry *n*-hexane (60 mL), tolyl hydrazine (2.74 g, 17.3 mmol) added, the mixture ooled to 0 °C,and NEt_3 (1.75 g, 17.3 mmol) dropwise added under agon atmosphere. After a period of 15 min,the ice bath was removed and the mixture was stirred at 20 °C for 4 h. The pale yellow residue (**8b**) was filtered off, washed with *n*-hexane (30 mL),and suspended in methanol (150 mL). o the well stirred suspension was dropwise added DBU (3.4 mL). After stirring for a few hours,the solution became dark red and a solid began to precipitate. After stirring for 5 days at 20 °C,the solid was filtered off and washed with 2-propanol. For purification, the solid was suspended in glacial acetic acid (10 mL) and stirred at 20 °C for 1.5 h. Subsequently, the solid was filtered off, suspended in an aqueous solution of sodium hydroxide (2%, 10 mL) and of ethanol (0.3 mL), and stirred at 20 °C for 1 h. The red dye was isolated by filtration and washed with water and, subsequently, with methanol: Yield 0.48 g (14%), dark red solid; IR (KBr) $\tilde{\nu}$ = 3419 (w), 1502 (s), 1446, 1396, 1315, 1293, 700 (m); ^{1}H NMR (TFA-d_1, 600 MHz) δ = 2.38 (s, 6 H), 5.85 (s, 1 H), 7.34 (m, 8 H), 7.45−7.47 (m, 4 H), 7.55−7.57 (m, 2 H), 7.99−8.00 (m, 4 H); UV−vis (DMF) λ_{max} (log ϵ) = 291 (4.61), 527 (4.33), 548 (4.35) nm; UV−vis (toluene) λ_{max} (log ϵ) = 292 (4.24), 303 (4.22), 525 (3.92), 553 (3.94) nm; UV−vis (CH_3CN) λ_{max} (log ϵ) = 288 (3.80), 523 (3.59), 544 (3.58) nm; UV−vis (acetic acid) λ_{max} (log ϵ) = 274 (4.59), 504 (4.32), 538 (4.43) nm; MS (EI, 70 eV) *m/z* (%) = 520 (37), 519 (100, $[M]^+$), 103 (10), 91 (16); HRMS (EI, 70 eV) calcd for $C_{33}H_{25}N_7$ 519.2166 (M^+), found *m/z* 519.2167 ± 2 ppm.

5,7-Diphenyl-3,9-di(4-tolyl)-hexaazaacridine (3c). A suspension of **6b** (2.28 g, 6.6 mmol) and PCl_5 (4.01 g, 19.3 mmol) in dry toluene (20 mL) was stirred under reflux for 2 h. The solvent and $POCl_3$ were removed under reduced pressure to give **7b**. The residue (**7b**) was suspended in dry *n*-hexane (60 mL), the mixture cooled to 0 °C, and phenyl hydrazine (1.7 mL, 16.0 mmol) dropwise added under an argon atmosphere. After a period of 15 min, the ice bath was removed and the mixture was stirred at 20 °C for 4 h. The pale yellow residue (**8c**) was filtered off, washed with *n*-hexane (30 mL), and suspended in methanol (200 mL). To the well stirred suspension was dropwise added DBU (3.4 mL). After stirring for a few hours, the solution became dark red and a solid began to precipitate. After stirring for 5 days at 20 °C, the solid was filtered off and washed with 2-propanol. For purification, the solid was suspended in glacial acetic acid (10 mL) and stirred at 20 °C for 1 h. Subsequently, the solid was filtered off, suspended in an aqueous solution of sodium hydroxide (4%, 10 mL) and of ethanol

(0.3 mL), and stirred at 20 °C for 1 h. The red solid was isolated by filtration, washed with water and 2-propanol, and dried at 100 °C: Yield 0.206 g (6%), red solid; IR (KBr) $\tilde{\nu}$ = 3428, 3054, 1594 (w), 1499 (s), 1396, 1301 (m), 1174, 1083, 1005, 863, 829, 776 (w); ^{1}H NMR (TFA-d_1, 600 MHz) δ = 2.34 (s, 6 H), 5.88 (s, 1 H), 7.29−7.52 (m, 14 H), 7.86 (m, 4 H); ^{13}C NMR (TFA-d_1, 150 MHz) δ = 15.7, 91.1, 119.9, 121.0, 122.3, 122.9, 125.7, 126.2, 127.7, 134.9, 141.4, 151.5, 151.9; UV−vis (AcOH) λ_{max} (log ϵ) = 283 (4.64), 542 (4.50) nm; UV−vis (CH_2Cl_2) λ_{max} (log ϵ) = 239 (4.11), 294 (4.73), 305 (4.75), 346 (3.91), 523 (4.42), 547 (4.51) nm; UV−vis (DMF) λ_{max} (log ϵ) = 294 (4.71), 525 (4.41), 548 (4.47) nm; UV−vis (toluene) λ_{max} (log ϵ) = 296 (4.67), 308 (4.71), 352 (3.64), 524 (4.35), 553 (4.43) nm; UV−vis (formic acid) λ_{max} (log ϵ) = 283 (4.63), 542 (4.50) nm; UV−vis (H_2SO_4) λ_{max} (log ϵ) = 226 (4.32), 341 (4.37), 451 (4.11), 685 (4.25) nm; fluorescence (DMF) $F_{\lambda max}$ (λ_{Ex}) = 585 (310) nm; MS (EI, 70 eV) *m*/*z* (%) = 520 (22), 519 (60, [M]$^+$), 117 (13), 77 (16); HRMS (EI, 70 eV) calcd for $C_{33}H_{25}N_7$ 519.2166 (M^+), found *m*/*z* 519.2164 ± 2 ppm.

5,7-Diphenyl-3,9-di(4-chlorophenyl)hexaazaacridine (3d). A suspension of **6c** (2.27 g, 6.6 mmol) and PCl_5 (4.01 g) in toluene (20 mL) was refluxed for 3 h. The workup, carried out as described for the synthesis of **7a**, afforded **7c**. The reaction of **7c** with phenyl hydrazine (1.7 mL) gave **8d** as described for the synthesis of **8a**. A methanol solution (250 mL) of **8d** and of DBU (3.4 mL) was stirred for 14 days at 20 °C. The solid was filtered off and washed with 2-propanol to give the crude product (0.862 g, 24%). For purification, the solid was suspended in glacial acetic acid (10 mL) and stirred at 20 °C for 1.5 h. Subsequently, the solid was filtered off, suspended in a mixture of an aqueous solution of sodium hydroxide (2%, 10 mL) and of ethanol (0.5 mL), and stirred at 20 °C for 1 h. The red solid was isolated by filtration, washed with water and, subsequently, with 2-propanol, and dried at 100 °C: Yield 0.833 g (23%), red solid; IR (KBr) $\tilde{\nu}$ = 3436 (m), 3095, 3060 (w), 1630, 1596, 1538 (m), 1497 (s), 1392, 1304, 1089, 1005, 861, 699 (m); ^{1}H NMR (TFA-d_1, 600 MHz) δ = 5.68 (s, 1 H), 7.41−7.42 (m, 8 H), 7.52 (m, 6 H), 7.97−7.99 (m, 4 H); ^{13}C NMR (TFA-d_1, 150 MHz) δ = 83.4, 119.9, 124.2, 125.0, 126.2, 127.5, 134.9, 135.0, 135.8, 151.5, 152.6; UV−vis (acetic acid) λ_{max} (log ϵ) = 280 (4.77), 537 (4.60) nm; UV−vis (DMF) λ_{max} (log ϵ) = 295 (4.81), 304 (4.80), 347 (3.90), 527 (4.53), 552 (4.50) nm; UV−vis (H_2SO_4) λ_{max} (log ϵ) = 225 (4.39), 287 (4.42), 342 (4.34), 454 (4.04), 667 (4.43) nm; fluorescence (DMF) $F\lambda_{max}$ (λ_{Ex}) = 579 (304) nm; MS (EI, 70 eV) *m*/*z* (%) = 563 (7, [M]$^+$, 2× ^{37}Cl), 562 (11), 561 (34, [M]$^+$, ^{37}Cl, ^{35}Cl), 560 (17), 559 (48, [M]$^+$, 2× ^{35}Cl), 180 (11), 137 (49), 77 (100); HRMS (EI, 70 eV) calcd for $C_{31}H_{19}Cl_2N_7$ *m*/*z* 559.1074 ([M]$^+$, 2× ^{35}Cl), found *m*/*z* 559.1064 ± 2 ppm.

5,7-Tolyl-3,9-di(4-chlorophenyl)hexaazaacridine (3e). A suspension of **6c** (2.55 g, 6.6 mmol) and PCl_5 (4.01 g) in toluene (20 mL) was refluxed for 2 h. The workup, carried out as described for the synthesis of **7a**, afforded **7c**. The reaction of **7c** with tolyl hydrazine (12.74 g, 7.3 mmol) and NEt_3 (1.75 g, 17.3 mmol) gave **8e** as described for the synthesis of **8c**. A methanol solution (250 mL) of **8e** and of DBU (2.7 mL) was stirred for 14 days at 20 °C. The precipitated solid was filtrated off, washed with 2-propanol, and recrystallized from chloroform: Yield 0.438 g (11%), dark red solid (chloroform); IR (KBr) $\tilde{\nu}$ = 3044, 1637, 1590 (w), 1499 (s), 1392 (m), 1299, 1088, 1005, 861, 831 (w); ^{1}H NMR (TFA-d_1, 600 MHz) δ = 2.35 (s, 6 H), 5.73 (s, 1 H), 7.27 (d, *J* = 7.5 Hz, 4 H), 7.32 (d, *J* = 7.5 Hz, 4 H), 7.41 (d, *J* = 8.4 Hz, 4 H), 7.96 (d, *J* = 8.4 Hz, 4 H); ^{13}C NMR (TFA-d_1, 150 MHz) δ = 14.6, 118.9, 123.4, 124.1, 124.3, 125.8, 131.7, 134.1, 135.0, 138.4, 150.8, 151.5; UV−vis (DMF) λ_{max} (log ϵ) = 295 (4.82), 304 (4.81), 529 (4.54), 553 (4.53) nm; UV−vis (CH_2Cl_2) λ_{max} (log ϵ) = 295 (4.87), 305 (4.87), 527 (4.57), 551 (4.59) nm; UV−vis (CH_3CN) λ_{max} = 292, 525, 546 nm; UV−vis (toluene) λ_{max} (log ϵ) = 297 (4.72), 308 (4.73), 528 (4.42), 556 (4.43) nm; UV−vis (ethanol) λ_{max} (log ϵ) = 293 (4.35), 301 (4.34), 524 (4.03), 547 (4.09) nm; UV−vis (acetic acid) λ_{max} (log ϵ) = 281 (4.80), 507 (4.53), 539 (4.63) nm; UV−vis (H_2SO_4) λ_{max} = 248, 323, 459, 681 nm; UV−vis (H_3PO_4) λ_{max} = 280, 537 nm; fluorescence (DMF) $F\lambda_{max}$ (λ_{Ex}) = 583 (555) nm; MS (EI, 70 eV) *m*/*z* (%) = 591 (7, [M]$^+$, 2× ^{37}Cl), 590 (11), 589 (29, [M]$^+$, ^{37}Cl, ^{35}Cl), 588 (17), 587 (38, [M]$^+$, 2× ^{35}Cl), 207 (28), 137 (51), 119 (51), 91 (50); HRMS (EI, 70 eV) calcd for $C_{33}H_{23}Cl_2N_7$ *m*/*z* 587.13865 ([M]$^+$, 2× ^{35}Cl), found *m*/*z* 587.14010 ± 2 ppm.

5,7-Diphenyl-3,9-di(4-nitrophenyl)hexaazaacridine (3f). A suspension of **6d** (2.69 g, 6.6 mmol) and PCl_5 (4.01 g) in toluene (20 mL) was refluxed for 2 h. The workup, carried out as described for **7a**, afforded **7d**. The reaction of **7d** with phenyl hydrazine (1.7 mL) afforded **8f** as described for the synthesis of **8c**. A methanol solution (400 mL) of **8f** and of DBU (2.7 mL) was stirred for 14 days at 20 °C. The precipitated solid was filtered off and washed with 2-propanol. For purification, the solid was suspended in acetic acid (10 mL) and stirred at 20 °C for 1.5 h. The red solid was isolated by filtration, washed with water and 2-propanol: Yield 0.542 g (14%), red solid; IR (KBr) $\tilde{\nu}$ = 3431 (m), 1629 (w), 1600 (m), 1499 (s), 1456, 1393 (m), 1345 (s), 1304 (m), 1235, 1213, 1170, 1070 (w), 1006, 857, 706 (m); ^{1}H NMR (TFA-d_1, 600 MHz) δ = 5.63 (s, 1 H), 7.42−7.54 (m, 10 H), 8.29−8.33 (m, 8 H); ^{13}C NMR (TFA-d_1, 150 MHz) δ = 82.5, 119.0, 119.1, 123.3, 125.4, 126.8, 133.1, 134.0, 135.1, 144.7, 150.8, 151.3; UV−vis (acetic acid) λ_{max} (log ϵ) = 280 (4.44), 500 (4.27), 534 (4.42) nm; UV−vis (DMF) λ_{max} (log ϵ) = 314 (4.58), 485 (4.28), 521 (4.40), 547 (4.34), 587 (4.10) nm; UV−vis (H_2SO_4) λ_{max} (log ϵ) = 227 (3.95), 274 (4.12), 328 (3.95), 485 (3.77), 631 (4.03) nm; UV−vis (H_3PO_4) λ_{max} = 284, 538 nm; fluorescence (DMF) $F\lambda_{max}$ (λ_{Ex}) = 610 (558) nm; MS (EI, 70 eV) *m*/*z* (%) 581 (6, [M]$^+$), 91 (7); HRMS (EI, 70 eV) calcd for $C_{31}H_{19}N_9O_4$ *m*/*z* 581.15545 (M^+), found *m*/*z* 581.15370 ± 2 ppm.

5,7-Tolyl-3,9-di(4-nitrophenyl)hexaazaacridine (3g). A suspension of **6d** (2.69 g, 6.6 mmol) and of PCl_5 (4.01 g) in toluene (20 mL) was refluxed for 2 h. The workup, carried out as described for **7a**, afforded **7d**. The reaction of **7d** with tolyl hydrazine (2.74 g, 17.3 mmol) afforded **8g** as described for the synthesis of **8c**. A methanol solution (250 mL) of **8g** and of DBU (2.7 mL) was stirred for 14 days at 20 °C. The precipitated solid was filtered off, washed with 2-propanol, and recrystallized from chloroform: Yield 0.428 g (11%), dark red solid (chloroform); IR (KBr) $\tilde{\nu}$ = 3426, 1602 (w), 1502 (s), 1392 (w), 1345 (s), 1302 (m), 1006 (w), 857 (w), 709 (w); ^{1}H NMR (TFA-d_1, 600 MHz) δ = 2.39 (s, 6 H), 5.69 (s, 1 H), 7.32 (d, *J* = 8.1 Hz, 4 H), .35 (d, *J* = 8.1 Hz, 4 H), 8.29 (d, *J* = 9.0 Hz, 4 H), 8.32 (d, *J* = 9.0 Hz, 4 H); ^{13}C NMR (TFA-d_1, 150 MHz) δ = 15.7, 119.9, 122.4, 122.9, 125.7, 126.2, 127.7, 134.9, 41.4, 151.5, 151.9; UV−vis (DMF) λ_{max} (log ϵ) = 315 (4.66), 524 (4.46); UV−vis (DCM) λ_{max} (log ϵ) = 240 (4.41), 310 (4.72), 481 (4.34), 522 (4.52), 543 (4.55), 582 (4.25) nm; UV−vis (toluene) λ_{max} (log ϵ) = 310 (3.72), 485 (3.38), 519 (3.46), 544 (3.59), 583 (3.38) nm; UV−vis (CH_3CN) λ_{max} (log ϵ) = 239 (3.99), 310 (4.28), 480 (3.94), 520 (4.07), 584 (3.78) nm; UV−vis (acetic acid) λ_{max} (log ϵ) = 280 (4.56), 501 (4.39), 536 (4.55) nm; UV−vis (H_2SO_4) λ_{max} = 228, 274, 345, 457, 649 nm; UV−vis (H_3PO_4) λ_{max} = 279, 335, 537 nm; fluorescence (DMF) $F\lambda_{max}$ (λ_{Ex}) = 600 (565) nm. $C_{33}H_{23}N_9O_4$ (609.604).

5,7-Diphenyl-3,9-dinaphthylhexaazaacridine (3h). A suspension of **6e** (2.76 g, 6.6 mmol) and of PCl_5 (4.01 g) in toluene (20 mL) was refluxed for 3 h. The workup, carried out as described for **7a**, afforded **7e**. The reaction of **7e** with phenyl hydrazine (1.7 mL) afforded **8h** as described for the synthesis of **8c**. An ethanol solution (500 mL) of **8h** and of DBU (3.4 mL) was stirred for 14 days at 20 °C. The precipiated solid was filtered off and washed with 2-propanol to give the crude product (0.823 g, 21%). For purification, the solid was suspended in acetic acid (10 mL) and stirred at 20 °C for 1.5 h. The solid was filtered off and suspended in a mixture of an aqueous solution of sodium hydroxide (2%, 10 mL) and of ethanol (0.3 mL) and stirred at 20 °C for 1 h. The red solid was isolated by filtration, washed with water and, subsequently, with 2-propanol, and dried at 100 °C: Yield 0.757 g (19%), red solid; IR (KBr) $\tilde{\nu}$ = 3056, 1593 (w), 1498 (s), 1398, 1350,

1296, 1232, 860, 762 (m); ^{1}H NMR (TFA-d_1, 600 MHz) δ = 5.54 (s, 1 H), 7.41−7.56 (m, 14 H), 7.81−8.10 (m, 8 H), 8.67 (m, 2 H); ^{13}C NMR (TFA-d_1, 150 MHz) δ = 85.5, 118.3, 119.9, 123.3, 123.4, 123.5, 124.6, 124.8, 125.0, 126.2, 127.6, 128.9, 131.6, 134.9, 152.2; UV−vis (acetic acid) λ_{max} (log ϵ) = 267 (4.80), 306 (4.71), 546 (4.64) nm; UV−vis (DMF) λ_{max} = 276, 315, 528, 557 nm; UV−vis (H_2SO_4) λ_{max} (log ϵ) = 217 (4.74), 262 (4.74), 310 (4.50), 460 (4.13), 663 (4.50) nm; MS (EI, 70 eV) *m*/*z* (%) 592 (23), 591 (51, $[M]^+$), 281 (11), 208 (14), 207 (61), 154 (16), 153 (98), 126 (20), 77 (28); HRMS (EI, 70 eV) calcd for $C_{39}H_{25}N_7$ *m*/*z* 591.2166 (M^+), found *m*/*z* 591.2163 ± 2 ppm.

5,7-Diphenyl-3,9-di(isonicotinoyl)hexaazaacridine (3i). A suspension of **6f** (2.11 g, 6.6 mmol) and of PCl_5 (4.01 g) was refluxed in toluene (20 mL) for 2 h. The workup, carried out as described for **7a**, afforded **7f**. The reaction of **7f** with phenyl hydrazine (1.7 mL) afforded **8i** as described for the synthesis of **8c**. An ethanol solution (300 mL) of **8f** and of DBU (3.7 mL) was stirred for 6 days at 20 °C. The precipitated solid was filtered off and washed with 2-propanol: Yield 0.891 g (27%), red solid; IR (KBr) $\tilde{\nu}$ = 3428, 3039, 1636, 1597 (w), 1501 (s), 1400, 1325, 1295, 857, 695 (m); ^{1}H NMR (TFA-d_1, 600 MHz) δ = 5.68 (s, 1 H), 7.43−7.44 (m, 4 H), 7.54−7.60 (m, 6 H), 8.70 (d, J = 6.9 Hz, 4 H), 8.90 (d, J = 6.9 Hz, 4 H); ^{13}C NMR (TFA-d_1, 150 MHz) δ = 84.8, 119.0, 119.9, 125.7, 127.5, 133.5, 137.0, 137.2, 145.3, 148.5, 151.9; UV−vis (DMF) λ_{max} (log ϵ) = 291 (4.72), 481 (4.28), 530 (4.49), 562 (4.25) nm; UV−vis (CH_2Cl_2) λ_{max} (log ϵ) = 237 (4.38), 288 (4.77), 477 (4.28), 527 (4.54), 559 (4.34) nm; UV−vis (CH_3CN) λ_{max} (log ϵ) = 236 (4.34), 287 (4.74), 476 (4.30), 525 (4.49), 556 (4.22) nm; UV−vis (acetone) λ_{max} (log ϵ) = 342 (3.64), 477 (4.07), 528 (4.24), 560 (4.02) nm; UV−vis (acetic acid) λ_{max} (log ϵ) = 269 (4.53), 521 (4.50) nm; UV−vis (toluene) λ_{max} (log ϵ) = 290 (4.36), 478 (3.90), 530 (4.11), 564 (3.98) nm; UV−vis (ethanol) λ_{max} (log ϵ) = 238 (4.39), 288 (4.86), 478 (4.29), 526 (4.51), 557 (4.28) nm; UV−vis (H_2SO_4) λ_{max} = 244, 381, 558 nm; UV−vis (H_3PO_4) λ_{max} (log ϵ) = 259, 485, 529 nm; fluorescence (DMF) $F\lambda_{max}$ (λ_{Ex}) = 583 (564) nm; MS (EI, 70 eV) *m*/*z* (%) 494 (22), 493 (57, $[M]^+$), 393 (11), 207 (47), 137 (46), 123 (74), 119 (50), 91 (37); HRMS (EI, 70 eV) calcd for $C_{29}H_{19}N_9$ *m*/*z* 493.17579 (M^+), found *m*/*z* 493.17789 ± 2 ppm.

5,7-Diphenyl-3,9-ditolylhexaazaanthracene (4b). The reaction of 4-toluoylchloride (15.50 g, 100.0 mmol), 1,3-diaminobenzene (5.40 g, 50.0 mmol), and NEt_3 (10.10 g, 100.0 mmol) in 200 mL of dichloromethane afforded, following the procedure as given for the synthesis of **6a**, *N*,*N*′-1,3-phenylenebis(4-methylbenzamide): Yield 9.60 g (56%), colorless prisms (ethanol), mp 216−217 °C; IR (KBr) $\tilde{\nu}$ = 3326 (m), 1646, 1607, 1541, 1490 (s), 1324, 1302 (m), 839, 777, 746, 679 (m); ^{1}H NMR (DMSO-d_6, 300 MHz) δ = 2.39 (s, 6 H), 7.27−7.35 (m, 5 H), 7.47−7.50 (m, 2 H), 7.88−7.91 (m, 4 H), 8.31−8.32 (m, 1 H), 10.20 (s, 2 H); ^{13}C NMR (DMSO-d_6, 150 MHz) δ = 21.0, 113.0, 116.0, 127.7, 128.5, 128.9, 132.1, 139.4, 141.5, 165.3; MS (EI, 70 eV) *m*/*z* (%) = 344 (0.2, $[M]^+$), 105 (1), 78 (2). $C_{22}H_{20}N_2O_2$ (344.41). The reaction of the bis(benzamide) (2.27 g, 6.6 mmol) with PCl_5 (4.01 g) in toluene (20 mL) afforded, following the procedure as given for the synthesis of **7a** (2 h reflux) the bis(imidoyl) chloride. The latter was reacted with phenyl hydrazine (1.7 mL), following the procedure as given for the synthesis of **8a**, to give the corresponding bis(amidrazone). The reaction of the latter with DBU (1.7 mL) in MeOH (150 mL), following the procedure as given for the synthesis of **3a**, afforded **4b**. Yield of the crude product: 0.629 g (18%). For purification, the solid was suspended in acetic acid (10 mL) and stirred at 20 °C for 1 h. The red solid was isolated by filtration and washed with water and, subsequently, with 2-propanol: Yield 0.338 g (10%), red solid; IR (KBr) $\tilde{\nu}$ = 3433 (m), 1594 (w), 1504 (s), 1397, 1308 (m), 1317 (s), 1176, 983, 856, 832, 765 (w); ^{1}H NMR (TFA-d_1, 600 MHz) δ = 2.32 (s, 6 H), 6.09, 6.10 (2 s, 2 H), 7.26−7.46 (m, 14 H), 7.67−7.68 (m, 4 H); ^{13}C NMR (TFA-d_1, 150 MHz) δ = 15.8, 88.6, 94.7, 118.7, 119.9, 122.4, 126.2, 126.3, 128.1, 135.2, 137.6, 143.0, 144.2, 145.3; UV−vis (AcOH) λ_{max} (log ϵ) = 315 (4.84), 391 (3.77), 411 (3.76), 568 (4.42) nm; UV−vis (DMF) λ_{max} (log ϵ) = 316 (4.84), 399 (3.79), 506 (4.26), 533 (4.41), 556 (4.47), 593 (4.29) nm; UV−vis (CH_2Cl_2) λ_{max} (log ϵ) = 278 (4.41), 316 (4.87), 328 (4.92), 399 (3.79), 533 (4.41), 554 (4.47), 591 (4.29) nm; UV−vis (toluene) λ_{max} (log ϵ) = 317 (4.83), 330 (4.91), 401 (3.80), 532 (4.37), 559 (4.41), 599 (4.29) nm; UV−vis (formic acid) λ_{max} (log ϵ) = 309 (4.81), 410 (3.96), 585 (4.37) nm; UV−vis (H_2SO_4) λ_{max} (log ϵ) = 259 (4.21), 325 (4.57), 426 (4.38), 719 (4.14) nm; fluorescence (DMF) $F\lambda_{max}$ (λ_{Ex}) = 395 (350) nm; MS (EI, 70 eV) *m*/*z* (%) 519 (38), 518 (100, $[M]^+$), 296 (12); HRMS (EI, 70 eV) calcd for $C_{34}H_{26}N_6$ *m*/*z* 518.2210 (M^+), found *m*/*z* 518.2210 ppm.

Acknowledgment. This work was supported by the Deutsche Forschungsgemeinschaft. A.B. thanks the state of Mecklenburg-Vorpommern for a scholarship. S.A. acknowledges scholarships from the Gottlieb Daimler- and Karl Benz-Stiftung and the DAAD. N.N.R.S. is grateful to the Dr. Gerda-von-Mach-Gedächtnisstiftung for a scholarship.

Note Added after ASAP Publication. Figure 18 was replaced, the corrected version was published June 4, 2008.

Supporting Information Available: X-ray data and crystallographic statistics for **3g**, experimental procedures for intermediates, spectroscopic results of the new compounds, copies of NMR spectra, the tables of computed optimized geometric parameters and energies, ^{13}C NMR chemical shifts, natural charge analyses for all species. This material is available free of charge via the Internet at http://pubs.acs.org.

JO8005123